Available online at www.sciencedirect.com
SCIENCE DIRECT®
Coordination Chemistry Reviews 249 (2005) 1811–1829
COORDINATION CHEMISTRY REVIEWS
www.elsevier.com/locate/ccr

Review

Pressure effect studies on spin crossover systems

Philipp Gütlich *, Vadim Ksenofontov, Ana B. Gaspar

Institut für Anorganische Chemie und Analytische Chemie, Johannes Gutenberg Universität, Staudinger Weg 9, D-55099 Mainz, Germany

Received 30 August 2004; accepted 14 January 2005
Available online 5 March 2005

Dedicated to Professor Jean Marie Lehn on the occasion of his 65th birthday.

Contents

Abstract

In the present review article we discuss the results of investigations of the influence of hydrostatic pressure (up to 1.2 GPa) on the spin transition behaviour in coordination compounds of 3d transition metal ions. The systems under investigation are mononuclear spin crossover compounds of iron(II) and chromium(II), dinuclear complexes of iron(II) exhibiting coexistence of intramolecular anti-ferromagnetic coupling and thermal spin crossover, and 1D, 2D and 3D polynuclear spin crossover complexes of iron(II). It is demonstrated that the application of hydrostatic pressure serves as a tool for modifying the ligand field strength in a controlled manner.

Keywords: Spin crossover; Pressure; Phase transitions; Hysteresis; Elastic interactions

1. Introduction

The effects of applied pressure on the spin crossover (SCO) phenomenon have already been studied by Ewald et

* Corresponding author. Tel.: +49 6131 3922 373; fax: +49 6131 3922 990.
E-mail address: guetlich@uni-mainz.de (P. Gütlich).

0010-8545/$ – see front matter © 2005 Elsevier B.V. All rights reserved.
doi:10.1016/j.ccr.2005.01.022

al. with a family of Fe(III) dithiocarbamate complexes in solution [1]. The low spin (LS) $^2T_2$ state has a smaller molecular volume than the high spin (HS) $^6A_1$ state and becomes favoured as pressure increases. König [2] pointed out that the strong dependence of the ligand-field strength on the metal-donor atom distances and the resulting large difference in metal–ligand bonds lengths between the two spin states leads to the change of entropy, which is the genuine driving force for the thermal spin transition (ST). Indeed, the underlying reason for the pressure influence on the spin transition process is the large difference in the metal–donor atom bond lengths, $\Delta r_{HL} = r_{HS} - r_{LS} \approx 0.1$ and 0.2 Å, for Fe(III) and Fe(II) spin crossover molecules, respectively. A schematic representation of the pressure influence on the LS and HS potential wells of Fe(II) is shown in Fig. 1: application of pressure increases the relative vertical displacement of the potential wells; the additional minor relative horizontal displacement of the potential wells due to a slight decrease in bond length with an increase in pressure has been neglected. Thus application of pressure favours the LS state of the molecule and shifts the spin transition to higher temperatures because pressure increases the zero point energy difference ΔE^0_{HL} by the work term $p\Delta V^0_{HL}$ and decreases the activation energy ΔW^0_{HL}, which finally favours the LS state.

Although the spin crossover phenomenon is essentially a property of the isolated complex molecule due to the competition between the dependence of the ligand-field strength on the metal–ligand bond length and the electron–electron repulsion, external perturbations such as pressure may effectively influence the spin crossover properties. Moreover, the application of pressure enables one to investigate the thermodynamic characteristics and microscopic aspects of the mechanism of spin transition in solids. Systematic and detailed studies of the concerted action of temperature and pressure variation on SCO compounds have only recently become possible with the development of special hydrostatic pressure cells in connection with magnetic susceptibility, optical and Mössbauer measurements, EXAFS and vibrational spectroscopy. The earlier, significant publications [3–13] cited in the review article [14a] published in 1994 refer to results obtained using mainly a Mössbauer high pressure cell. Much progress has been made since then. In the following we shall discuss significant results of pressure effect studies on solid SCO systems reported during the last decade. Among them are mononuclear SCO systems of iron(II) and chromium(II), dinuclear complexes of iron(II) exhibiting a fascinating interplay between thermal SCO and anti-ferromagnetic coupling, and polymeric 1D, 2D and 3D SCO compounds of iron(II).

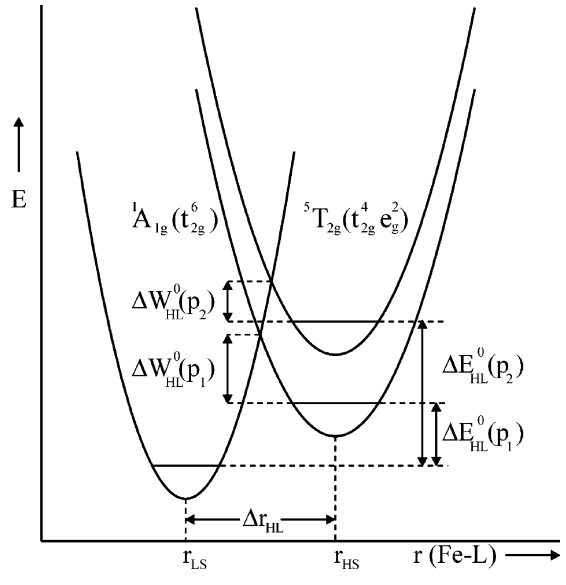

Fig. 1. Schematic representation of the pressure influence ($P_2 > P_1$) on the LS and HS potential wells of Fe(II). The minor change in bond lengths Δr_{HL} under pressure is not considered, (adapted from [33]).

2. Experimental methods and previous pressure effect studies

In most SCO coordination compounds [14b] the molecular and lattice structures can be relatively easily disrupted by shear deformations, which always occur when applied pressure is not hydrostatic. Crystal defects may also be caused by non-hydrostatic pressure and influence the SCO behaviour. Mechanically treated polycrystalline SCO compounds confirm that with increasing milling the residual HS fraction increases, the transition curves become broader and hysteresis loops widen and flatten out [15]. Comparison of the results from pressure effect studies of the same compound under non-hydrostatic [16] and hydrostatic conditions [17], has shown that non-hydrostatic pressure of ≅0.1 GPa can significantly deform the transition curve (partial suppression of the SCO process).

In many investigations of the effect of pressure on SCO systems a high pressure cell was used in connection with Mössbauer spectroscopy. For optimal performance the cell should be constructed with windows made of hard material which is transparent to γ-radiation. Gas (e.g. He, Ar) or liquid is generally used as the pressure-transmitting medium. Such a hydrostatic gas pressure cell operating at pressures up to ≤0.2 GPa was applied in Mössbauer experiments on [Fe(2-pic)$_3$]Cl$_2$·EtOH (2-pic = 2-(aminomethyl)pyridine) [12]. A newly developed Mössbauer pressure cell made of hardened beryllium bronze and equipped with windows made of B_4C and using oil as the pressure transmitting medium has been described in [18] and is shown in Fig. 2. It is suitable for measurements up to 1.4 GPa in the temperature range of 2–400 K. The diamond anvil cell (DAC) technique is used for measurements of Mössbauer spectra up to ≈50 GPa [19]. Pressure calibration is accomplished by focusing a blue or green laser on a small chip of ruby within the pressure medium of the DAC. The major disadvantages of this cell for Mössbauer spectral studies are the small capacity of the sample holder, requiring the use of isotopically enriched samples, and the non-hydrostatic pressure. For instance, it is likely that the

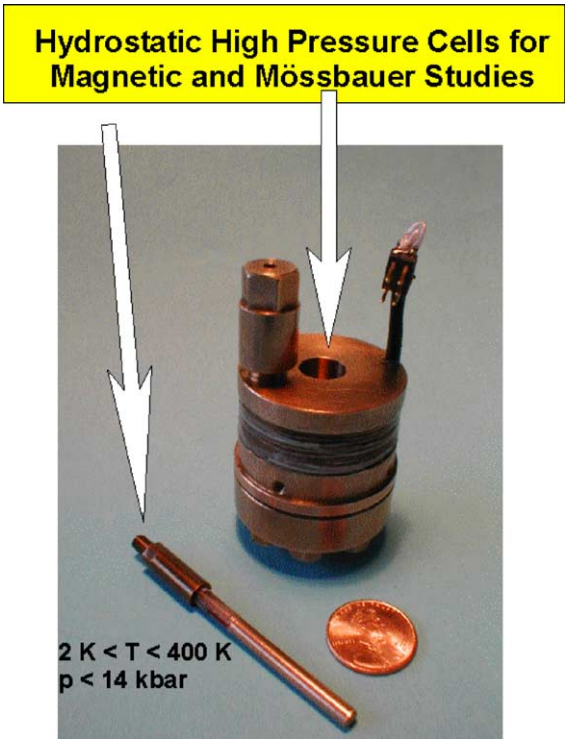

Fig. 2. High pressure cells for Mössbauer and magnetic measurements (14 kbar corresponds to 1.4 GPa).

non-hydrostatic nature of the pressure is responsible for the unusual partial LS → HS transformation in $Fe[HB(pz)_3]_2$ (pz = 1-pyrazolyl) observed at pressures above 4 GPa [9,19].

Transparency of diamonds to photons over a wide energy range from infrared to X-rays allows wide application of the DAC technique. A pressure cell with a beryllium gasket between two diamonds, containing a hole of ≈0.3 mm diameter for encapsulating a sample with a liquid as pressure-transmitting medium, provides hydrostatic pressure conditions up to 1.0 GPa. It has proven to be a very efficient device for X-ray diffraction studies and is being employed by several groups in X-ray crystal structure determinations of SCO compounds under pressure [20–22]. High-pressure X-ray absorption spectroscopy for the study of spin crossover phenomena in several Fe(II) and Co(II) tris(pyrazolyl)borate complexes has also been reported [23,24].

A pressure effect study with infrared spectroscopy of several thiocyanato and isocyanato complexes of Fe(II) showed that the spin transitions occurred below 1.0 GPa [25]. The application of Raman spectroscopy for samples under high pressure was recently reported [26]. In this study, pressure-induced hysteresis at room temperature was found for spin crossover polymers of formula $\{Fe(pz)[M(CN)_4]\}\cdot 2H_2O$ (pz = pyrazine and M = Ni, Pd, Pt). An experimental set-up for temperature- and pressure-dependent optical absorption spectroscopy was reported in [27]. A helium gas pressure cell for pressures up to 0.1 GPa has been described in conjunction with a closed-cycle He refrigerator, allowing variable temperatures between 15 and 300 K. Hydrostatic He pressure was created by a two-membrane pneumatic compressor. This installation has been successfully used to study several iron(II) SCO systems, where comparatively low external pressures induced significant changes in the thermodynamic equilibrium as well as in the relaxation dynamics. A low-temperature helium pressure chamber operating in the pressure range up to 0.16 GPa for optical reflectivity studies is described in [28]. This apparatus is particularly useful for the study of spin crossover processes occurring in thin layers or on the surface of solid SCO materials.

Magnetic susceptibility measurements on SCO compounds at elevated pressures are possible with a hydrostatic high pressure cell made of hardened beryllium bronze and using silicon oil as a pressure-transmitting medium [17,29]. The cell has the following characteristics: range of pressure up to ≈1.4 GPa, with an accuracy of ±0.025 GPa. The sample holder is ≈1 mm in diameter and 5–7 mm in length and operates in the temperature range of 1.5–400 K. Because of the small weight and the negligible magnetic background, the cell can be used in Foner-type and SQUID magnetometers. The pressure is calibrated using the superconducting transition temperature of high purity tin. Fig. 2 shows this hydrostatic pressure cell, which has been used in our susceptibility measurements discussed in the following.

3. Effect of pressure on mononuclear spin crossover systems

Most of the SCO compounds of iron(II) consist of mononuclear FeN_6 core complex molecules held together in the crystal lattice by non-covalent interactions. They display a wide range of spin crossover behaviour from gradual to abrupt transitions with and without thermal hysteresis [14]. In the following we shall discuss results of pressure effect studies on SCO systems displaying both gradual and abrupt transitions with and without hysteresis and of pressure induced spin crossover in a compound that does not undergo thermal SCO at ambient pressure.

3.1. Effect of pressure on $[Fe(phen)_2(NCS)_2]$

$[Fe(phen)_2(NCX)_2]$ (X = S, Se) are the first and still among the most extensively studied SCO systems of iron(II) [30] (Fig. 3a)). Fisher and Drickamer [31] investigated the effect of pressure on the spin transition behaviour of this system using the Mössbauer effect. Their results demonstrated not only the expected increase of HS → LS conversion with increasing pressure at a given temperature, but even a partial reverse LS → HS transformation above a certain threshold of pressure. Subsequent studies of Adams et al. [4] and Pebler [5] did not confirm the reverse LS → HS process, raising the question about the presence of hydrostatic conditions in the experiments carried out by Fisher and Drickamer. The first magnetic susceptibility measurements under pressure on the title compound were carried out by Usha et al. [7]. All the

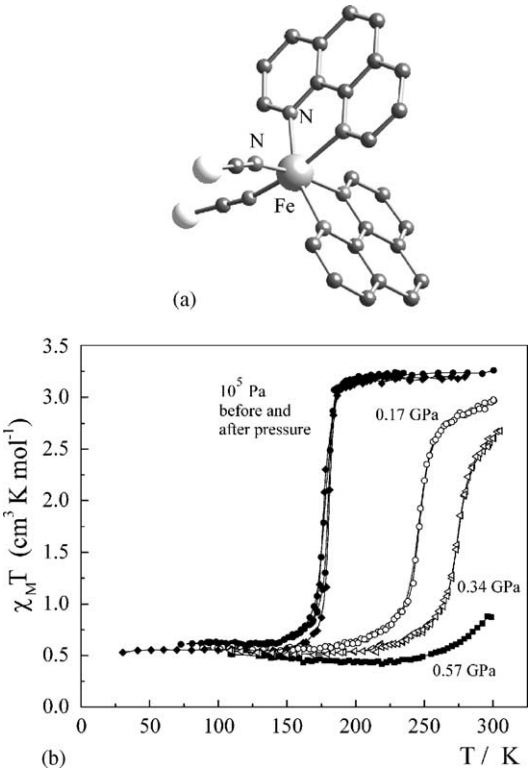

Fig. 3. Molecular structure (a) and $\chi_M T$ vs. T curves at different pressures for [Fe(phen)$_2$(NCS)$_2$] polymorph II (b), (adapted from [33]).

results obtained in these studies provided the evidence for HS → LS conversion under pressure, the reported values of the critical pressure $P_{1/2}$ for 50% spin state conversion at room temperature ranging between 0.6 and 1.2 GPa. König et al. have demonstrated the existence of two crystallographic modifications of [Fe(phen)$_2$(NCS)$_2$] [30]. Polymorph I undergoes an almost complete thermal spin transition, whereas in polymorph II a fraction of HS molecules of ca. 17% is retained at low temperatures. A possible reason for the range of $P_{1/2}$ values indicated above is that the studies were carried out with different polymorphs. While in reference [4] the actual polymorph that was investigated is not specified, in [5] and [31] the experiments were carried out on polymorph II. The non-hydrostatic nature of the pressure in the experiments using diamond anvil cells could also contribute to the discrepancy in $P_{1/2}$ values. X-ray diffraction on a single crystal of polymorph II did not reveal a change of the space group, neither during the thermal spin crossover nor under pressure up to 1.3 GPa [32(b)]. A very recent magnetic susceptibility study under hydrostatic pressure [33] is presented in the following.

The $\chi_M T$ versus T curves measured for [Fe(phen)$_2$(NCS)$_2$] polymorph II at different pressures are shown in Fig. 3b). At ambient pressure the transition curve is extremely steep with $T_{1/2}$ = 177 K. The presence of a narrow temperature hysteresis and the value of residual HS fraction (≅17%) are in agreement with published data [32(a)]. As the pressure is increased, the transition curve is displaced to higher temperatures with an average dependency of 220 K GPa^{-1}. With the application of pressure the narrow hysteresis loop disappears and the transition curves become gradual. At pressures around 0.6 GPa the sample is mostly in the LS state up to room temperature, however, the residual HS fraction below the transition remains essentially unaltered. This is in line with results found in [32 (b)], viz., conservation of the space group during the spin crossover transition under pressure up to 1.3 GPa and the structure being a decisive factor for the completeness of the spin transition in [Fe(phen)$_2$(NCS)$_2$]. It should be noted that usually a complete spin transition is accomplished under hydrostatic pressure. A progressive diminution of the pressure influence on the transition temperature ($\partial T_{1/2}/\partial P$ = 410 K GPa^{-1} at 0.17 GPa, 180 K GPa^{-1} at 0.34 GPa, 150 K GPa^{-1} at 0.57 GPa) points at the presence of a steric barrier, which can be a possible factor preventing a complete HS → LS transformation in polymorph II of [Fe(phen)$_2$(NCS)$_2$]. In fact, π-interactions between [Fe(phen)$_2$(NCS)$_2$] units are found within the (*a*,*b*) layers and, more precisely, these interactions are oriented in the *b* direction [22]. The pressure dependence of the lattice parameters *a*, *b* and *c*, reveals a significant discontinuity for *a*, but quasi-linear behaviour for *b* and *c*. The discontinuity along *a* seems to be related to the spin state change, as a similar effect has been observed in the dilatation experiments [22]. Finally, a comparison between the evolution of the unit cell volume and the $\chi_M T$ product under pressure clearly shows the correlation between the magnetic and structural properties for this compound.

The influence of pressure on the thermodynamic parameters of the HS ↔ LS transition in [Fe(phen)$_2$(NCS)$_2$] interpreted in the frame of a phenomenological mean-field description [34] is given in Section 4. This compound appears to be ideal for this purpose, because of the proven absence of a structural phase transition in both temperature and pressure variation.

3.2. Spin crossover under pressure in [$CrI_2(depe)_2$]

The compound *trans*-bis[1,2–bis(diethylphosphino)ethane]di-iodochromium(II) ([CrI$_2$(depe)$_2$]) (Fig. 4a)) is the first chromium(II) compound exhibiting thermal spin crossover reported by Halepoto et al. [35]. It shows a very sharp $^3T_{1g}$ (S = 1) ↔ ^5E_g (S = 2) spin transition with $T_{1/2}$ = 169 K without noticeable thermal hysteresis at ambient pressure. A magnetic susceptibility study under pressure shows a progressive increase of $T_{1/2}$ and a decrease of the transition steepness with increasing pressure (Fig. 4b) [33]. Pressure of ca. 0.8 GPa transforms the compound entirely to the low-spin state at ambient temperature. Qualitatively, one can interpret this pressure effect on the grounds of mean-field theory [34]. In mean field approximation the pressure dependence of the spin transition temperature obeys the Clausius–Clapeyron relation:

$$\frac{\partial T_{1/2}}{\partial P} = \frac{\Delta V}{\Delta S_{HL}} \quad (1)$$

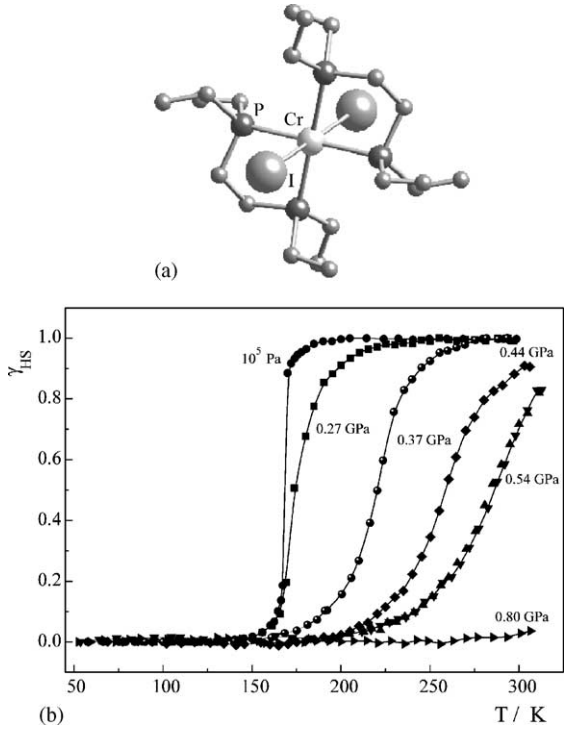

Fig. 4. Molecular structure (a) and spin transition curves γ_{HS} (T) at different pressures for $[CrI_2(depe)_2]$ (b), (adapted from [33]).

This relation reflects the scaling of the transition temperature $T_{1/2}$ and the volume change ΔV. Fig. 5 shows the plots of $T_{1/2}$ versus pressure for $[Fe(phen)_2(NCS)_2]$ polymorph II and $[CrI_2(depe)_2]$. For the latter compound strong non-linearity contrasts the almost linear dependence for $[Fe(phen)_2(NCS)_2]$. A detailed interpretation of this is not possible without the knowledge of the thermal and pressure dependences of the elementary cell volume of $[CrI_2(depe)_2]$, as has been accomplished for $[Fe(phen)_2(NCS)_2]$ [22]. However, it looks as though the elementary cell volume of

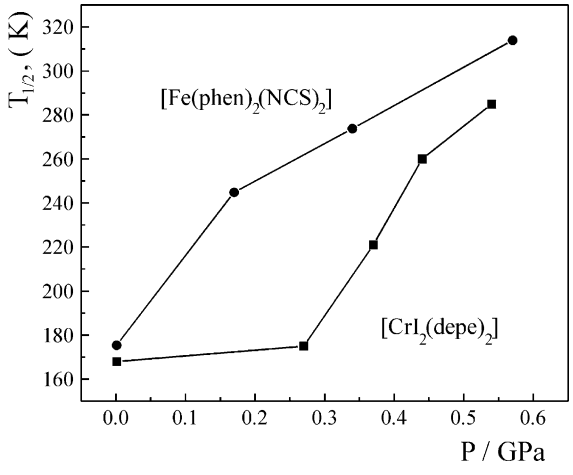

Fig. 5. Plot of $T_{1/2}$ vs. P for $[Fe(phen)_2(NCS)_2]$ and $[CrI_2(depe)_2]$, (adapted from [33]).

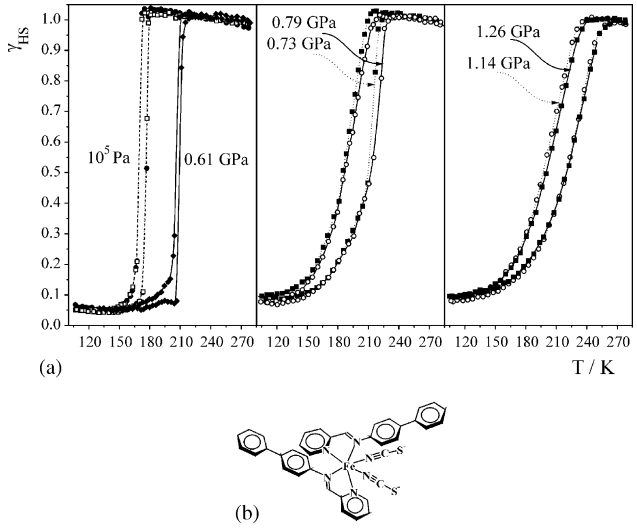

Fig. 6. Plot of γ_{HS} vs. T at different pressures for $[Fe(PM\text{-}Bia)_2(NCS)_2]$ (a) and molecular structure (b), (adapted from [37]).

$[CrI_2(depe)_2]$ hardly changes across the spin transition in the pressure range up to ≈0.3 GPa, similar to the observations in X-ray studies on $[Fe(mtz)_6](BF_4)_2$ after LIESST effect at ambient pressure [36]. The reason may be found in the different compressibilities of the large iodide ions as compared to the smaller and harder phosphorus donor atoms in the CrP_4I_2 core. Application of low pressure seems to reduce mainly the volumes of the iodide ions leaving the Cr–P donor atom distances essentially unchanged. The influence of pressure on $T_{1/2}$ in the present case seems to start above a certain threshold when the Cr–P bond lengths are noticeably altered by pressure.

3.3. *Effect of pressure on the abrupt spin transition with hysteresis in $[Fe(PM\text{-}Bia)_2(NCS)_2]$ and on the gradual transition in $[Fe(PM\text{-}Pea)_2(NCS)_2]$*

In Fig. 6 are depicted the plot of γ_{HS} versus T at different pressures for the complex $[Fe(PM\text{-}Bia)_2(NCS)_2]$ (PM-Bia = (*N*-(2′-pyridylmethylene)-4-aminobiphenyl) together with the molecular structure [37]. At atmospheric pressure an almost complete and unusually abrupt transition (within 1–2 K) is observed with hysteresis of 5 K width. When the pressure is increased up to ca. 0.60 GPa, the transition temperature $T_{1/2}$ is shifted upwards and the width of the hysteresis loop is reduced. At higher pressures the hysteresis width reaches approximately 25 K. At 1 GPa, the spin transition is more gradual and the hysteresis width diminishes slightly. Further increase of pressure around 1.3 GPa has no further effect. The formation of this large hysteresis for $P > 0.6$ GPa is totally reversible, as illustrated by the identical data obtained at atmospheric pressure before (open squares) and after (filled circles) the application of hydrostatic pressure up to 1.26 GPa. This suggests the formation of a new crystallographic phase at elevated pressure, denoted as phase II; whereas the observed one at low pressure is denoted as phase

I [37]. The transition behaviour in the 0.6–0.8 GPa range reflects the presence of a mixture of the original phase I and the pressure-induced phase II. Both phases show the typical features of first-order transitions. The observation that the hysteresis becomes much broader in the pressure-induced phase II lends support to the conclusion that in the new phase II the spin transition is accompanied by a crystallographic phase change. Also, it seems that the strength of the cooperative interactions between the spin state changing molecules has no direct influence on the hysteresis width. The steepness of the transition curves, which is a measure of the cooperativity, is reduced in the pressure-induced phase II, but the hysteresis width is approximately 10 times larger than in phase I. The spin crossover process in phase I of $[Fe(PM\text{-}Bia)_2(NCS)_2]$ is not accompanied by a change of the space group, which is *Pccn* above and below $T_{1/2}$.

For the mononuclear compound $[Fe(PM\text{-}Aza)_2(NCS)_2]$ (PM-aza = (*N*-(2′-pyridyl-methylene)-4-(azophenyl)aniline) [37], γ_{HS} at ambient pressure decreases continuously with decreasing temperature corresponding to a gradual and complete spin transition (Fig. 7). An increase of pressure shifts the transition temperature upwards and decreases the slope of the transition curve. The pressure dependence of $T_{1/2}$ is linear, the slope of the $T_{1/2}$ versus P straight line, $dT_{1/2}/dP = 160\,K\,GPa^{-1}$, is very close to that observed for the mononuclear compounds $[Fe(2\text{-}pic)_3]Cl_2$ EtOH (2-pic = 2-picolylamine) [12] and $[Fe(abpt)_2(NCS)_2]$ [41] where $dT_{1/2}/dP = 150$ and $176\,K\,GPa^{-1}$, respectively. This pressure influence on gradual transitions can be qualitatively interpreted on the basis of the phenomenological theory of phase transitions in spin crossover systems [12]. On these grounds the slope of the spin transition curve decreases under pressure and $T_{1/2}$ shifts upwards. The thermal dependence of γ_{HS} for the compound $[Fe(PM\text{-}Aza)_2(NCS)_2]$ under pressure demonstrates these features.

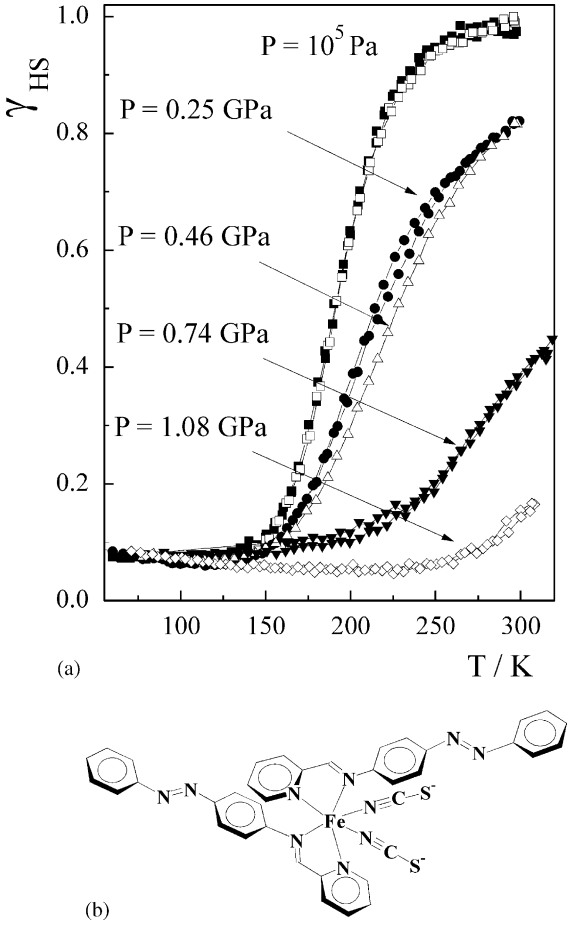

Fig. 7. Plot of γ_{HS} vs. T at different pressures for $[Fe(PM\text{-}Aza)_2(NCS)_2]$ (a) and molecular structure (b), (adapted from [37]).

3.4. Pressure-induced complete spin transition in $[Fe(mtz)_6](BF_4)_2$ with non-equivalent metal centers

A pressure effect study was carried out on the mononuclear complex $[Fe(mtz)_6](BF_4)_2$ (mtz = 1-methyl-tetrazole) [38] in which the iron(II) ions occupy two non-equivalent crystallographic sites A and B with population ratio 1:1 [36]. At ambient pressure only site A molecules undergo thermal spin transition, whereas the molecules in site B remain in the HS state down to 4.2 K [39]. The ^{57}Fe Mössbauer spectra of $[Fe(mtz)_6](BF_4)_2$ above ~160 K, however, show only one quadrupole doublet typical of iron(II) in the HS state. This obviously indicates that the two sites A and B are only minutely different in energy. Poganiuch et al. [40] have shown that at low temperatures the ground state of iron(II) in both sites can be converted by light into long-lived metastable spin states: the LS state of A site molecules to HS with green light, this process being called $LIESST(LS \rightarrow HS)_A$, and the HS state of B site molecules to LS with red light, denoted as $LIESST(HS \rightarrow LS)_B$.

Fig. 8 shows the temperature dependence of the HS fraction γ_{HS} at different pressures derived from susceptibility measurements. At ambient pressure $T_{1/2} = 75$ K, in accor-

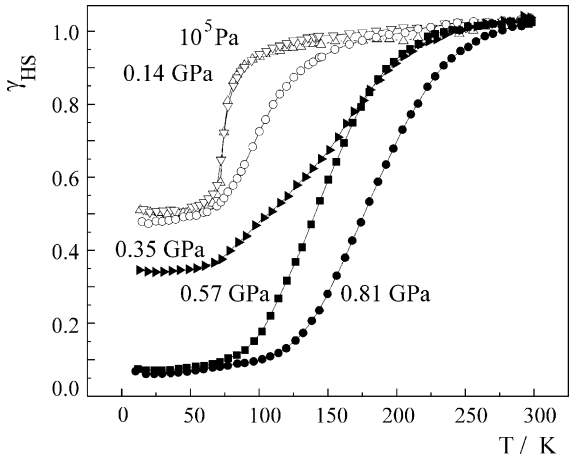

Fig. 8. Plot of γ_{HS} vs. T at different pressures for $[Fe(mtz)_6](BF_4)$, (adapted from [38]).

dance with previous measurements [40]. The absence of thermal hysteresis and the value of the residual HS fraction of ~50% also agree with published data [40]. At a pressure of ca. 0.14 GPa, the slope of the transition curve decreases and the transition shifts to higher temperatures. One should notice that this pressure modifies the spin transition behaviour associated with A site molecules but does not change the spin state of B site molecules. This correlates with observations made in an X-ray study [36] where practically no change of volume during LIESST $(HS \rightarrow LS)_B$ was found. According to the Clausius–Clapeyron relation (1), the effects of external pressure will be minimal if $\Delta V = 0$. However, higher pressure of 0.35 GPa not only shifts the part of the curve associated with A site molecules upwards, but also causes partial spin transition of B site molecules which is clearly seen in the lowering of $\gamma_{HS}(T)$ in the low temperature region. Pressure of 0.57 GPa switches the rest of B site molecules from HS to LS and the spin transition in $[Fe(mtz)_6](BF_4)_2$ becomes nearly complete. The highest applied pressure of 0.81 GPa generates a gradual transition curve with $T_{1/2} \sim 180$ K.

3.5. Pressure-induced spin transition in the paramagnetic [Fe(abpt)$_2$(NCS)$_2$] polymorph B

Fig. 9 shows the temperature dependence of the $\chi_M T$ product of $[Fe(abpt)_2(NCS)_2]$ polymorph B (abpt = 4-amino-3,5-bis(pyridin-2-yl)-1,2,4-triazole) at different pressures and a perspective view of the molecular structure [41]. At room temperature and at atmospheric pressure the complex is high spin. As the temperature is lowered, $\chi_M T$ practically remains constant and the sharp decrease of $\chi_M T$ at temperatures below 25 K is caused by zero-field splitting of the HS iron(II) ions. This behaviour remains as pressure is increased up to 0.44 GPa, but an incomplete thermal spin crossover appears around $T_{1/2} = 65$ K. It is reasonable to assume that a slow kinetics blocks the HS ↔ LS equilibrium, due to the low temperatures involved in the spin transition of $[Fe(abpt)_2(NCS)_2]$ below 0.44 GPa. A relatively sharp spin transition takes place at $T_{1/2} = 106$, 152 and 179 K, as pressure increases to 0.56, 0.86 and 1.05 GPa, respectively. The pressure dependence of $T_{1/2}$ is nearly linear and similar as observed for $[Fe(2\text{-pic})_3]Cl_2$ EtOH [12]. The application of hydrostatic pressure to $[Fe(abpt)_2(NCS)_2]$ has once more demonstrated the principal possibility of inducing thermal spin crossover in a HS compound by altering the ligand field strength in a controlled manner, and thereby shifting the ΔE_{HL} parameters (see Fig. 1) from negative to positive values.

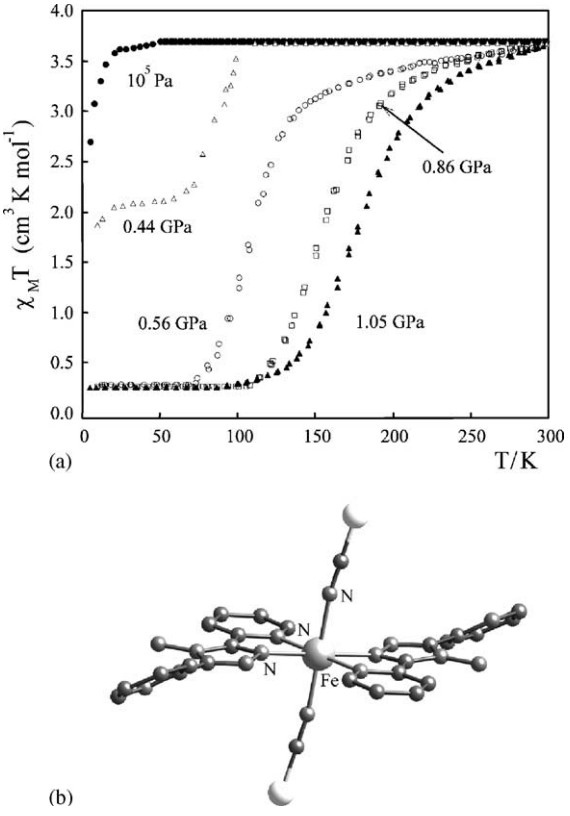

Fig. 9. $\chi_M T$ vs. T curves at different pressures for $[Fe(abpt)_2(NCS)_2]$ (a) and molecular structure (b), (adapted from [41]).

3.6. The influence of hydrostatic pressure on the hysteresis width in [Fe(phy)$_2$(BF$_4$)$_2$]

Mössbauer studies on the first-order spin transition in $[Fe(phy)_2](BF_4)_2$ and $[Fe(phy)_2](ClO_4)_2$ under pressure [16] revealed an increase of the hysteresis widths with increasing pressure contrary to the expectation from mean field theory [34]. In these experiments, samples were pressed between two disks of boron carbide using a tin metal gasket. Such a pressure cell construction does not guarantee hydrostatic pressure conditions so that the unexpected increase of the width of the hysteresis loop could be connected with a large uniaxial component of applied stress. The observed irreversible changes of the residual HS fraction at low temperatures in $[Fe(phy)_2](ClO_4)_2$ is most probably due to the formation of defects in polycrystalline samples as a consequence of non-hydrostatic conditions. In order to confirm the reported unexpected increase of the width of the hysteresis loop under pressure the spin transition in this compound was re-investigated under hydrostatic pressure conditions [17]. The results are displayed in Fig. 10.

In Fig. 11 the measured transition temperatures $T_{1/2}\downarrow\uparrow$ and the mean value $T_{1/2} = 1/2(T_{1/2}\downarrow + T_{1/2}\uparrow)$ are plotted versus pressure together with the Mössbauer data obtained by König et al. [16]. Up to 0.12 GPa, both sets of data agree well. The straight lines are linear regressions in the range up to 0.39 GPa and 0.44–0.58 GPa. Below 0.39 GPa the average temperature $T_{1/2}$ increases by 30 K GPa^{-1} (broken line in Fig. 11) and the hysteresis width $\Delta T_{1/2}$ increases. The discontinuity of $T_{1/2}\uparrow$ around 0.41 GPa possibly indicates a pressure-induced crystallographic phase transition. The temperature $T_{1/2}\uparrow$ remains constant whereas, $T_{1/2}\downarrow$ decreases slightly with increasing pressure.

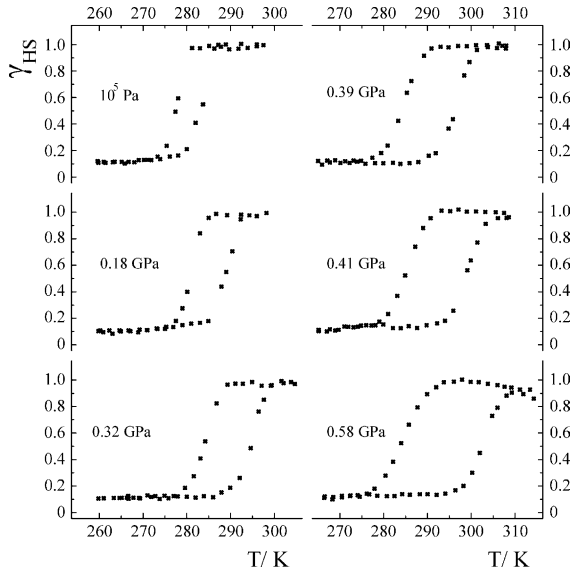

Fig. 10. Plot of γ_{HS} vs. T at different pressures for $[Fe(phy)_2](BF_4)_2$, (adapted from [17]).

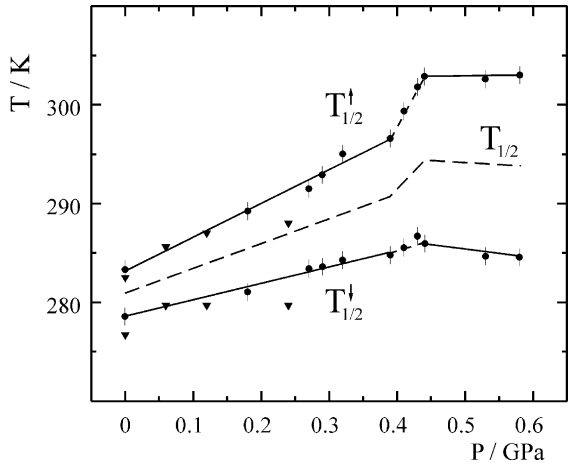

Fig. 11. Transition temperatures $T_{1/2}\downarrow\uparrow$ and the mean value $T_{1/2} = T_{1/2}\downarrow + T_{1/2}\uparrow$ for $[Fe(phy)_2](BF_4)_2$ are plotted vs. pressure. The triangles represent the measurements of König et al. [16], (adapted from [17]).

4. Theoretical description of the pressure effect in isotropic spin crossover compounds

On thermodynamical grounds, thermally induced spin crossover is described in terms of Gibbs free energy within the regular solution theory [3,12,14,17]. The pressure effect on the spin crossover behaviour is determined by the magnitude of the volume change of the unit cell per spin crossover complex, ΔV, and by the intermolecular interaction free energy F_{int} (γ,T). The change of the Gibbs free energy at an external pressure P is given by:

$$\Delta G = \Delta F_{HL} + F_{int}(\gamma, T) - TS_{mix}(\gamma) + \gamma P \Delta V \quad (2)$$

γ is the fraction of HS molecules and ΔF_{HL} the change of the free energy due to the spin transition. The mixing entropy is given by the expression:

$$S_{mix}(\gamma) = -k_B[\gamma \ln \gamma + (1-\gamma)\ln(1-\gamma)] \quad (3)$$

In mean-field approximation the interaction energy can be expanded in the following form:

$$F_{int}(\gamma, T) = \Delta_s \gamma - \Gamma \gamma^2 \quad (4)$$

The parameter Γ describes the interaction between HS and LS complexes; the lattice energy shift Δ_s depends upon their interaction with the reference lattice [34].

The change of the free energy may be expressed as:

$$\Delta F_{HL}(T) = \Delta H(T_{1/2}) - \Delta S_{HL} T \quad (5)$$

Here, $\Delta H(T_{1/2})$ and ΔS_{HL} are the changes of the enthalpy and the entropy at ambient pressure. Under the condition that the lattice is in thermal equilibrium,

$$\left(\frac{\partial \Delta G}{\partial \gamma}\right)_{T,p} = 0 \quad (6)$$

Finally, the pressure influence on the spin crossover is described by the equation of state

$$T = \frac{(\Delta H(T_{1/2}) + \Delta_s + P\Delta V - 2\gamma\Gamma)}{(k_B \ln(1-\gamma/\gamma) + \Delta S_{HL})} \quad (7)$$

Applying Eq. (7) to the data of the magnetic susceptibility measurements under pressure for $[Fe(phen)_2(NCS)_2]$ several important thermodynamical features have been drawn. Assuming, according to [34], Δ_s being independent of temperature, one can extract the volume changes ΔV per spin crossover complex. The resulting average change of the unit cell volume of 134 Å^3 is comparable with the value of 119 Å^3 found in the structural study of the $[Fe(phen)_2(NCS)_2]$ polymorph II under pressure [22]. The slight difference may be attributed to a possible pressure influence on the energy shift Δ_s. With increasing pressure the transition curves become more gradual (Fig. 3(b)). It can be understood, considering the so-called reduced pressure introduced by Köhler et al. [12]:

$$\Pi^* = \frac{\Delta F_{HL}(T) + \Delta_s + P\Delta V}{\Gamma}, \quad (8)$$

which characterizes the type of the spin crossover transition [12]. A first order transition with hysteresis is expected to occur at temperatures

$$T_{1/2} < T_c = \frac{\Gamma}{2k_B} \quad (9)$$

if $\Pi^*(T_c) < 1$; the spin transition is of continuous type if $\Pi^*(T_c) > 1$. At $P = 10^5$ Pa the reduced pressure is $\Pi^* = 0.62$. As a consequence, a first-order transition with a very steep transition curve is observed. One can estimate that at an external pressure $P \geq 0.05$ GPa the parameter Π^* exceeds 1,

giving rise to gradual transitions. The observation of smooth transition curves at $P \geq 0.17$ GPa confirms this conclusion.

A detailed thermodynamical treatment of the spin transition under the influence of external pressure was reported for $[Fe(ptz)_6](PF_6)_2$ (ptz = 1-*n*-propyltetrazole) [27]. This compound shows a rather steep transition with strong cooperativity, but without hysteresis. The interaction constant $\Gamma = 101\ cm^{-1}$ was found to be very close to the critical value above which hysteresis solely due to the cooperative effects is expected. In contrast to the case of $[Fe(phen)_2(NCS)_2]$ polymorph II, the interaction constant was found to be pressure independent presumably because of the comparatively low pressure applied in this study.

The increase of the hysteresis width with increasing pressure in $[Fe(phy)_2](BF_4)_2$ contradicts the expectation following from the phenomenological mean field theory of phase transitions in SCO compounds [34]. In the frame of this approach the pressure dependence of the spin transition temperature given by relation (1) predicts an increasing transition temperature with increasing pressure. Furthermore, the mean field approach predicts a decrease of the hysteresis width and of the slope of the transition curve with increasing pressure [7,12,34(c)]. The hysteresis vanishes at a critical pressure, and at even higher pressures the transition transforms to the gradual type belonging to the overcritical region of the phase diagram. A shift of the transition temperature and a decrease of the slope of the gradual transition were observed in $[Fe(2\text{-pic-}ND_2)_3]Cl_2EtOD$ [12]. The data were obtained by Mössbauer measurements under hydrostatic pressures up to 0.15 GPa using a helium gas pressure cell. The expected decrease of the width of the hysteresis loop with increasing pressure was observed in $[Fe(bt)_2(NCS)_2]$ [42]. But the above-mentioned pressure effects on the spin transition in $[Fe(phy)_2](BF_4)_2$ and also in $[Fe(PM\text{-}Pea)_2(NCS)_2]$ [37], are not in line with a mean field approach [34]. The parallel shift of the two-step transition curve and the behaviour of the hysteresis width (Fig. 12) observed for the SCO compound [Fe(5-NO_2-sal-*N*(1,4,7,10))] under pressure [43] also cannot be adequately described by this theory.

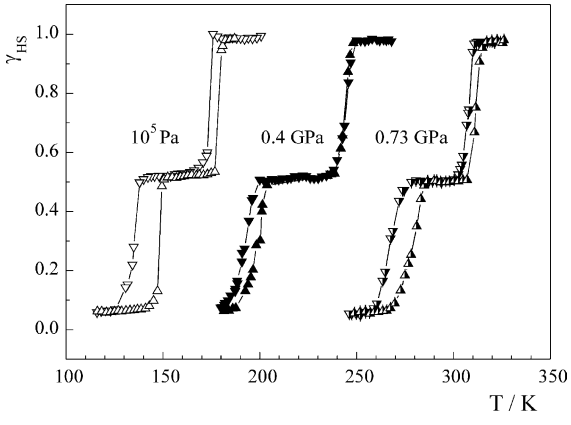

Fig. 12. Plot of γ_{HS} vs. T at different pressures for [Fe(5-NO_2-sal-N(1,4,7,10))], (adapted from [38]).

A possible explanation for increasing hysteresis width under applied pressure has been suggested by Das and Ghos [44], who discuss the Landau expansion of the free energy density with third- and fifth-order couplings between elastic strains and the order parameter of the phase transition. However, this theory cannot be mapped on the free energy of a spin crossover system, because it contains, on the one hand, no linear term of the order parameter which is the dominant one in the free energy of a spin crossover system, and on the other hand no direct coupling exists between the pressure and the order parameter. The direct coupling is given by the experimental fact that there is a volume change of the crystal proportional to the fraction of molecules of either spin states. The mean field approach by Köhler et al. [12] neglects all indirect couplings of the pressure to the order parameter, which was chosen to be the fraction γ_{HS} of HS molecules.

In order to describe the pressure effect on hysteresis and the scope of the above-mentioned experimental features of spin transitions, the mean field approximation of the free energy for spin crossover compounds has been extended [17]. For the interpretation of the interaction constants on the basis of elasticity theory the indirect coupling of pressure to the order parameter through the pressure dependence of the bulk modulus has been taken into account [45].

Using the theoretical considerations of [17] and taking into account only the linear terms in the expansion of the difference of the free energies of HS and LS states around T_c (Eq. (4)) the following expressions for the pressure derivatives of the transition temperature $dT_{1/2}/dP$ and hysteresis width $d\sqrt{\Delta T_{1/2}}/dP$ have been derived:

$$\frac{dT_{1/2}}{dP} = (2\gamma^G + 1)\frac{T_c}{K}\left(\frac{A}{\sigma_c} + \frac{T_{1/2}}{T_c}\right) \tag{10}$$

$$\frac{d\sqrt{\Delta T_{1/2}}}{dP} = (2\gamma^G + 1)\frac{\sqrt{T_c}}{K}\left(\tau_c A + \frac{1}{2}\sqrt{\frac{\Delta T_{1/2}}{T_c}}\right) \tag{11}$$

The quantity A is a function of physical parameters of the compounds:

$$A = \frac{3\gamma_0 - 1}{2\gamma_0}\frac{K}{2\gamma^G + 1}\frac{\Delta V}{2k_B T_c} + \frac{\Delta_s - 2k_B(T_c + \sigma_c T_{1/2})}{2k_B T_c} \tag{13}$$

where $\tau_c = d\sqrt{\Delta T^*_{1/2}}/d\Pi^*$ depends on the reduced hysteresis width $\Delta T^*_{1/2} = \Delta T_{1/2}/T_c$ and the reduced pressure Π^* (Eq. (8)). Eqs. (10) and (11) show that the derivatives $dT_{1/2}/dP$ and $d\sqrt{\Delta T_{1/2}}/dP$ are linear functions of the variable A, which depends on $T_{1/2}$ and T_c, on the molecular volume change between HS and LS species ΔV, the dimensionless parameter σ_c which is the entropy change ΔS_{HL} divided by $2k_B$, and the ratio $K/(2\gamma^G + 1)$, whereas K is the bulk modulus, γ^G the Grüneisen parameter and γ_0 the Eshelby constant [46]. Thus one can conclude that the different behaviour of $T_{1/2}$ and $\Delta T_{1/2}$, even the unexpected decrease of $T_{1/2}$ and also the increase of $\Delta T_{1/2}$with increasing pressure, is explained by the different values of the parameter A. The calculated val-

ues of the parameter A, the boundaries of changes of $T_{1/2}$ and $\Delta T_{1/2}$ for several spin crossover compounds are presented in [47].

Summarizing, the increase of the width of the hysteresis in $[Fe(phy)_2](BF_4)_2$ with increasing pressure can be described in mean field theory of spin transitions if the dependence of the bulk modulus K on pressure is introduced. The parameters entering the theory have values comparable to those found in other spin crossover compounds, thus giving a consistent picture. This theory qualitatively describes the behaviour of $T_{1/2}$ and $\Delta T_{1/2}$ under pressure but does not always give realistic values for the physical parameters of the investigated iron(II) compounds. To clarify the reasons for such discrepancies, further investigations on SCO compounds with a systematic definition of the above mentioned experimental parameters K, Δ_s, γ^G, etc., are necessary.

5. Effect of pressure on dinuclear spin crossover systems

Closely associated with the goal of designing and preparing new multifunctional materials [48], the idea of combining different electronic properties, like magnetic exchange and spin transition, in one and the same system emerged. One of the steps along this line aimed to afford a multi-property material began with the class of 2,2′-bipyrimidine (bpym)-bridged iron(II) dinuclear compounds (Fig. 13) [49].

A remarkable feature of the spin crossover process in several dinuclear iron(II) compounds is a plateau in the two-step transition curve. These macroscopic steps, also detected by means of Mössbauer spectroscopy and calorimetric measurements, were interpreted in terms of a microscopic two-step transition between the three possible spin pairs of each individual dinuclear molecule [50]: [HS–HS] ↔ [HS–LS] ↔ [LS–LS].

The pressure dependence of the thermal variation of $\chi_M T$ has proved to be a useful diagnostic probe to show that the formation of [HS–LS] spin pairs is not

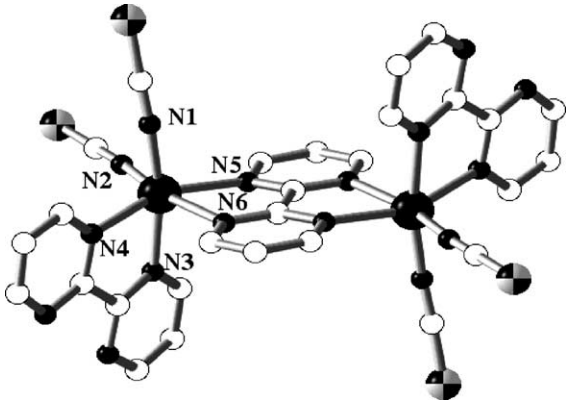

Fig. 13. Molecular structure of {[Fe(bpym)(NCS)$_2$]$_2$(bpym)]}, (adapted from [49]).

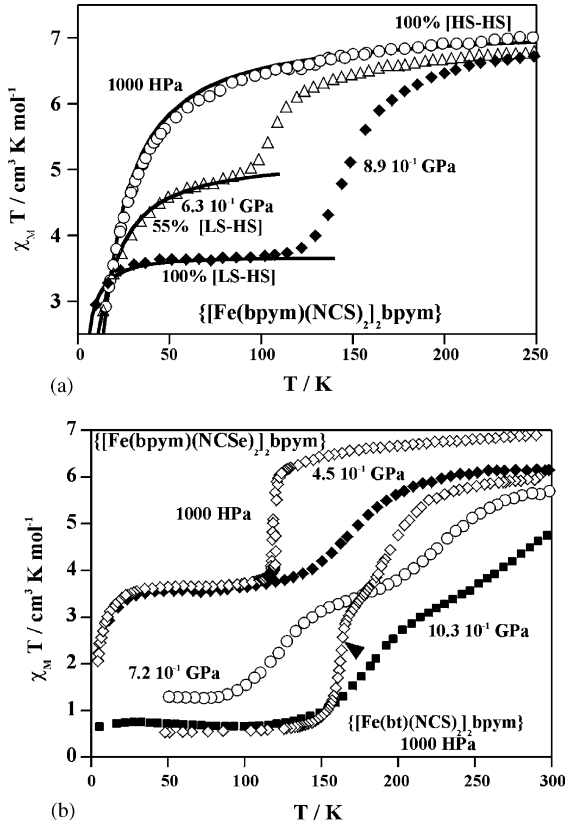

Fig. 14. Temperature dependence of $\chi_M T$ for {[Fe(bpym)(NCS)$_2$]$_2$(bpym)} at different pressures (a). The solid lines, together with estimated concentrations of [HS–LS] and [HS–HS] species correspond to calculations using the appropriate Hamiltonian. Temperature dependence of $\chi_M T$ for {[Fe(bpym)(NCSe)$_2$]$_2$(bpym)} at different pressures (b). The magnetic behaviour of {[Fe(bt)(NCS)$_2$]$_2$(bpym)} at room pressure has been also included for comparison, (adapted from [49]).

fortuitous but that they are the preferentially formed species in the dinuclear-type complexes [51]. Two members of the {[Fe(L)(NCX)$_2$]$_2$bpym} family have been examined: {[Fe(L)(NCS)$_2$]$_2$bpym} and {[Fe(L)(NCSe)$_2$]$_2$bpym}. Fig. 14 displays the thermal dependence of $\chi_M T$ at different pressures. At ambient pressure, and over the whole temperature range, {[Fe(L)(NCS)$_2$]$_2$bpym}contains only the anti-ferromagnetically coupled [HS–HS] pairs (Fig. 14a). Co-existence of anti-ferromagnetic coupling and spin crossover in {[Fe(L)(NCS)$_2$]$_2$bpym} clearly follows from magnetic susceptibility measurements at $P = 0.63$ GPa. When the pressure is increased to 0.63 GPa a partial conversion from 100% [HS–HS] to 55% [HS–LS] species takes place. The incompleteness of spin conversion is due to the fact that at low temperatures the spin conversion is so slow that the HS state becomes metastable. Thus anti-ferromagnetically coupled [HS–HS] pairs and [HS–LS] uncoupled pairs become co-existent in {[Fe(L)(NCS)$_2$]$_2$bpym}at 0.63 GPa, as reflected in the thermal dependence of $\chi_M T$. Finally, for $P = 0.89$ GPa total conversion to [HS–LS] pairs is accomplished. At this pressure, {[Fe(L)(NCS)$_2$]$_2$bpym}undergoes a similar [HS–HS] ↔ [HS–LS] spin transition at $T_{1/2} \approx 150$ K as in

{[Fe(L)(NCSe)$_2$]$_2$bpym}at ambient pressure. The effect of pressure on the thermal dependence of the spin state of {[Fe(L)(NCSe)$_2$]$_2$bpym} seems to be a decrease in the degree of cooperativity reflected in the more gradual $\chi_M T$ function as compared to that under ambient pressure and a shift of $T_{1/2}$ towards higher temperatures for pressures lower than 0.45 GPa (Fig. 14b). For higher pressures, a second transition appears in addition to the former one, due to the onset of thermal ST in the second metal centre. Between 0.72 and 1.03 GPa a two-step ST function is observed.

From the analysis of the results of the pressure experiments, it is inferred that a plateau results from successive ST in the two metal centres, leading first to the formation of relatively stable [HS–LS] pairs and then, above a critical pressure, to the formation of [LS–LS] pairs on further lowering of the temperature. The intermolecular interactions between [HS–LS] pairs leads to domains that contribute to the stability of the crystal lattice. The pressure induced low-temperature state of {[Fe(L)(NCS)$_2$]$_2$bpym}consisting almost entirely of the [HS–LS] units is stable at least up to 1.1 GPa. For {[Fe(L)(NCSe)$_2$]$_2$bpym}, a pressure of 0.45 GPa shifts $T_{1/2}$ by ca. 50 K upwards without increasing the amount of the LS fraction. Only at higher pressures does the second step appear for this derivative. These observations underline the role of intermolecular interactions in the stabilisation of the hypothetical "chequerboard-like" structure consisting of [HS–LS] units as proposed by Spiering and co-workers [12].

In order to investigate the competition between magnetic interaction and spin transition in {[Fe(L)(NCS)$_2$]$_2$ bpym}quenching experiments have been performed at 0.63 GPa [52]. Fig. 15 displays the magnetic behaviour of the quenched sample at increasing temperatures. It can be inferred from the thermal dependence of $\chi_M T$ that [HS–HS] entities can be frozen in as a metastable state at low temperatures. Heating the sample above ca. 60 K leads to re-formation of the stable state, which, in this temperature regime, consists mostly of [HS–LS] dinuclear species. Two main factors, namely, anti-ferromagnetic intramolecular interactions and elastic interactions, are believed to play an important role in the stabilisation of the metastable state. Considering the low value of $J \approx -4.1\ cm^{-1}$ of the former one in comparison with the decay temperature of $T \approx 60$ K and the unusually slow kinetics of the relaxation to the stable state, as compared to the relatively fast kinetics of spin transitions taking place at higher temperature, one can conclude that the relaxation is an essentially thermally activated process and that the crystal lattice is substantially involved. It is the structural rearrangement, associated with the spin changing process, that is responsible for the trapping of the [HS–HS] metastable species and not the magnetic interactions. If the magnetic interactions were responsible, the dynamics of the relaxation to the stable state would be much faster. In other words, elastic interactions rather than magnetic coupling drive the transformations of [HS–HS] ↔ [HS–LS] under pressure.

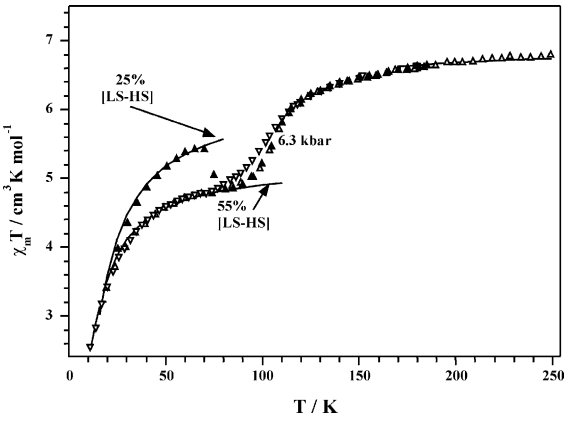

Fig. 15. Quenching experiment at 0.63 GPa (6.3 kbar): a sample of {[Fe(bpym)(NCS)$_2$]$_2$(bpym)} was cooled from 300 K to 4.2 K with a cooling rate of ca. 100 K min^{-1} and then warmed up to 300 K at 2 K min^{-1} (filled triangles). The subsequent warming (filled triangles) reveals that a substantial fraction of the HS centres does not convert into the LS state showing the occurrence of magnetic coupling in the additional [HS–HS] pairs. Thermal relaxation to the equilibrium state takes place at ca. 70 K, (adapted from [49]).

6. Effect of pressure on 1D, 2D and 3D polymeric spin crossover systems

Many one- two- and three-dimensional SCO have been synthesised and characterized during the last decade ([22,53] and references therein). In the following we shall discuss the pressure studies carried out on several kinds of such materials with the aim to arrive at a deeper insight into the cooperative interactions in polymeric SCO systems. They bear the potential of practical applications because of the strong cooperative regimes as well as the thermochromic effects associated to their spin transitions.

6.1. 1D spin crossover systems

The first one-dimensional (1D) polymeric spin crossover compound, which was reported by Lavrenova and co-workers [54] and re-investigated by Kahn and co-workers [55,56], belongs to the family of [Fe(4-*R*-trz)$_3$](anion)$_2$·*x*H$_2$O (4-*R*-trz = 4-substituted 1,2,4-triazole). In this system the iron atom is triple-bridged by triazole ligands through the nitrogen atoms occupying the 1- and 2-positions and defining a linear chain (Fig. 16a). The ST behaviour depends on the substituent in position 4, the counterion and the non-coordinating solvent molecules. Some of these compounds show very abrupt spin transitions close to room temperature and with thermal hysteresis of width up to 35 K. Studies of the effect of pressure on the spin transition in some of these complexes reveal remarkable features relevant to possible applications as pressure sensors.

The system [Fe(hyptrz)$_3$](4-chlorophenylsulfonate)·H$_2$O where hyptrz = 4-(3′-hydroxpropyl)-1,2,4-triazole [57] shows a very steep and complete ST around 180 K with thermal hysteresis of 6 K width as evidenced by magnetic

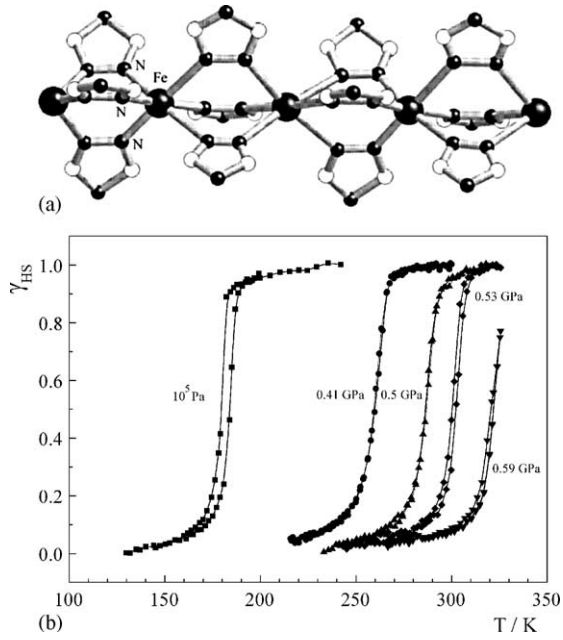

Fig. 16. Structure of the polymeric $[Fe(triazole)_3]_n^{2+}$ spin crossover cation deduced from EXAFS data [56] (a) and plot of γ_{HS} vs. T at different pressures for $[Fe(hyptrz)_3]$(4-chlorophenylsulfonate)·H_2O (b), (adapted from [38]).

susceptibility measurements at ambient pressure (Fig. 16b). Applying pressure induces a parallel shift of the transition curve up to room temperature and even above. This parallel shift is unusual as one generally observes a flattening of the transition curves with increasing pressure. Furthermore, it is interesting that the width of the hysteresis loop behaves non-monotonically with increasing pressure. Fig. 17 shows the pressure dependence of the LS fraction, γ_{LS}, at 290 K. A very sharp HS → LS transition is observed at room temperature around ∼0.6 GPa which is accompanied by an easily detectable colour change from white to deep purple. This feature could be used for applications in a pressure sensor.

Similar pressure effect studies have been performed on $[Fe(hyetrz)_3]$(4-chlorophenylsulfonate) [58] leading to the same type of behaviour for the $\chi_M T$ versus T curves under pressure (Fig. 18). Moreover, the thermal hysteresis width, 10 K was nearly independent of pressure. The strength of the cooperativity, however, apparently is not altered as in the previous case. The experimental results suggest that the hysteresis originates not only from intrachain but also from interchain interactions. The pressure influence is more pronounced in these systems than in mononuclear compounds. Thus the $dT_{1/2}/dP$ slopes are found as 240 and 230 K GPa^{-1} for $[Fe(hyptrz)_3]$(4-chlorophenylsulfonate)·H_2O and $[Fe(hyetrz)_3]$(4-chlorophenylsulfonate), respectively, compared to 150 K GPa^{-1} reported for $[Fe(2\text{-}pic)_3]Cl_2$·EtOH [12], 176 K GPa^{-1} for $[Fe(abpt)_2(NCS)_2]$ and 160 K GPa^{-1} for $[Fe(PM\text{-}Aza)_2(NCS)_2]$.

Another class of one-dimensional spin crossover systems concerns the complexes of formula $[Fe(L)(bt)(NCS)_2]$·bt

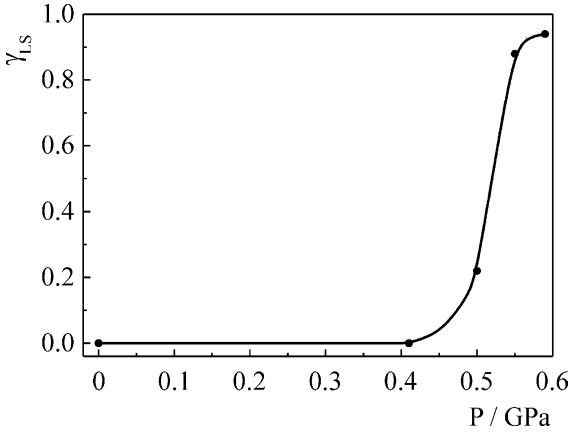

Fig. 17. Pressure dependence of the LS fraction, γ_{LS}, for $[Fe(hyptrz)_3]$(4-chlorophenylsulfonate)·H_2O at 290 K, (adapted from [57]).

where L = 4,4′-bipyridine (4,4′-bipy) [59], 4,4′-azopyridine (azpy) [60], bt = 2,2′-bi-thiazoline. As depicted in Fig. 19, these compounds consist of parallel linear chains defined by *trans*-4,4′-bipy or *trans*-azpy linked to iron(II) ions. For $[Fe(4,4'\text{-}bipy)(bt)(NCS)_2]$ the crystal structure is made up by crystallographically independent parallel chains associated to slightly different $[FeN_6]$ cores (see Fig. 19). In the

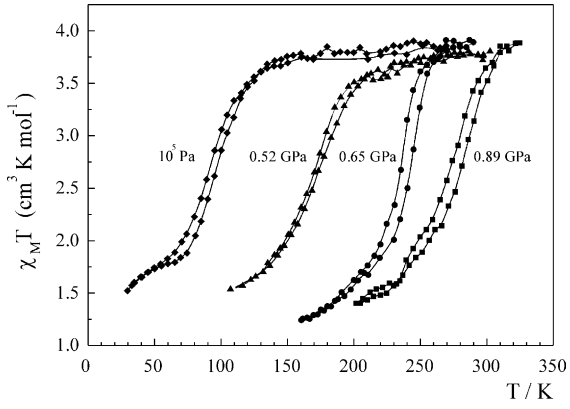

Fig. 18. Plot of γ_{HS} vs. T at different pressures for $[Fe(hyetrz)_3]$(4-chlorophenylsulfonate), (adapted from [58]).

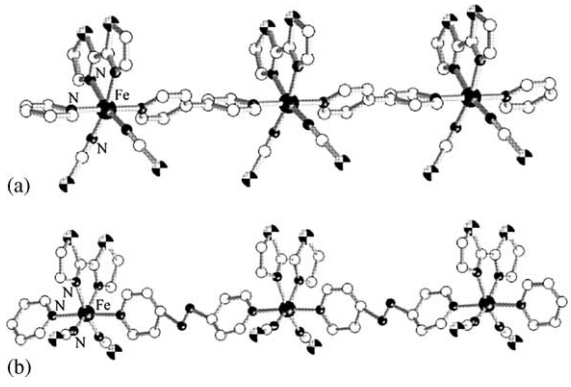

Fig. 19. Views of the chains $[Fe(4,4'\text{-}bipy)(bt)(NCS)_2]$ (a) and $[Fe(azpy)(bt)(NCS)_2]$·bt (b), (adapted from [59,60]).

case of [Fe(azpy)(bt)(NCS)$_2$]·bt only one type of Fe(II) crystallographic site was found. The equatorial plane is defined by two nitrogen atoms of one bt ligand and two thiocyanate groups in *cis* position for both complexes. The coordination octahedron of the iron(II) is strongly distorted in both cases.

The magnetic behaviour of these derivatives shows that a very incomplete spin transition occurs in[Fe(4,4′-bipy)(bt)(NCS)$_2$], while [Fe(azpy)(bt)(NCS)$_2$]·bt is paramagnetic in the whole range of temperatures at atmospheric pressure. The incomplete character of the spin transition in [Fe(4,4′-bipy)(bt)(NCS)$_2$] is a consequence of the low temperatures at which the conversion takes place. For temperatures lower than ca. 70 K the kinetics of the HS → LS process becomes very slow and quenches the spin transition. This behaviour can be understood in the frame of a simple Ising-like model [59]. In Fig. 20 are depicted the $\chi_M T$ versus T curves at different pressures for [Fe(4,4′-bipy)(bt)(NCS)$_2$]. It is remarkable that the incompleteness of the spin transition persists even at 0.97 GPa where the percentage of HS molecules deduced from the molar susceptibility value at 60 K is ca. 50%. Kinetic effects seem to be responsible for the slow HS → LS conversion below 70 K for all applied pressures. The decrease of the magnetic susceptibility below 50 K is due to ZFS (zero field splitting) of the iron(II) ions remaining in the HS state. $T_{1/2}$ moves upwards with increasing pressure. The experimental transition curves at all pressures can be fairly well fitted with a Boltzmann function which points at the presence of non cooperative interactions in this system. As shown in Fig. 20b, the pressure studies on [Fe(azpy)(bt)(NCS)$_2$]·bt evidences a similar behaviour of $\chi_M T$ versus T as observed for [Fe(4,4′-bipy)(bt)(NCS)$_2$]. But the influence of pressure seems to be somewhat less pronounced as can be seen from a comparison of the spin transition curve at 0.3 GPa in Fig. 20a with that at 0.56 GPa in Fig. 20b. Both are very similar regarding the shape and extent of spin state conversion at comparable temperatures. The fact that it needs higher pressure in the latter case than in the former together with the fact that no spin transition is seen in the latter case over the whole temperature range at atmospheric pressure is indicative of a weaker ligand field strength operative in the system with azpy bridging ligand as compared to that with bipy bridges.

Another example of pressure induced spin crossover behaviour in 1D systems is the compound [Fe(bpym)(NCS)$_2$] [51]. The $\chi_M T$ versus T plot in Fig. 21b shows that at ambient pressure this complex is HS in the whole range of temperature. As in the dinuclear analogue [Fe(bpym)(NCS)$_2$]$_2$bpym [49–52] the magnetic behaviour is dominated by intramolecular magnetic exchange mediated by the bpym bridge, which extends along the 1D system (Fig. 21a). However, [Fe(bpym)(NCS)$_2$] undergoes noticeable thermal spin transition at pressures much higher than in the case of

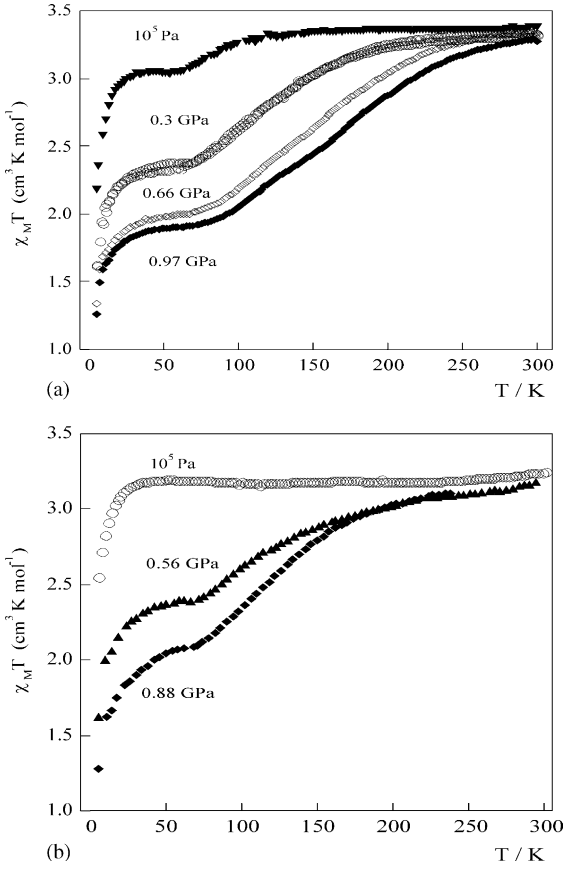

Fig. 20. $\chi_M T$ vs. T curves at different pressures for [Fe(4,4′-bipy)(bt)(NCS)$_2$] (a) and [Fe(azpy)(bt)(NCS)$_2$]·bt (b), (adapted from [60]).

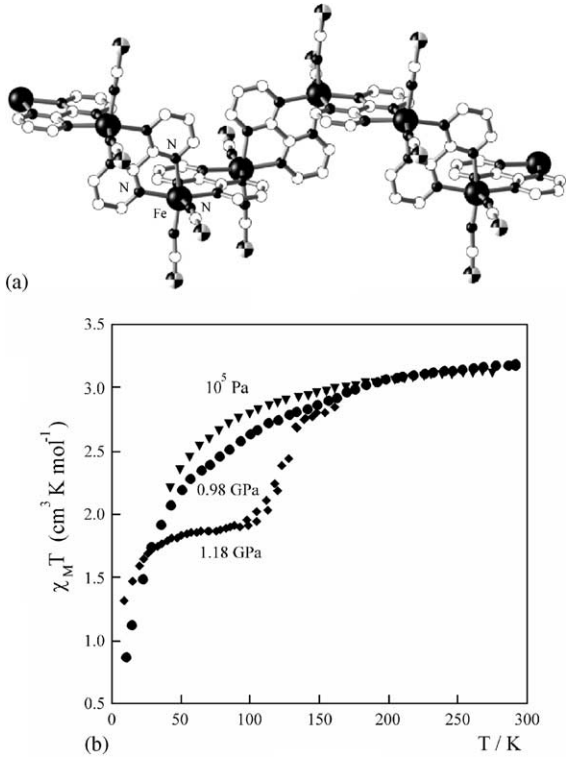

Fig. 21. Molecular structure of the polymeric complex [Fe(bpym)(NCS)$_2$] (a) and $\chi_M T$ vs. T curves at different pressures for [Fe(bpym)(NCS)$_2$] (b), (adapted from [51]).

$[Fe(bpym)(NCS)_2]_2bpym$. As can be seen in Fig. 21b, the curve measured at 0.98 GPa shows no indication of spin crossover; at 1.18 GPa, however, there is partial spin transition between 100 and 150 K involving 50% of iron(II) centers. The significantly higher pressures required to trigger the spin transition in $[Fe(bpym)(NCS)_2]$ compared to $[Fe(bpym)(NCS)_2]_2bpym$ are rather surprising in view of their molecular structures. The average Fe–N bond distances can be considered the same in both compounds (2.180 and 2.179 Å for $[Fe(bpym)(NCS)_2]_2bpym$ and $[Fe(bpym)(NCS)_2]$, respectively), and consequently, the ligand field strength is expected to be very similar in both compounds. So, the difference in sensitivity to pressure should be attributed to different packing of active SCO centres in the crystal lattice.

A microscopic model describing the role of hydrostatic pressure on spin crossover in one-dimensional systems was developed by Klokishner et al. [61]. The system Hamiltonian includes long- and short-range interactions and takes into account external pressure. Long-range interactions are shown to arise from the coupling of the electronic states of the Fe(II) ion to the full symmetric strain. Short-range interactions are also introduced in the model. The short-range interactions of a crossover molecule with two nearest neighbours in the chain is only considered. It is shown that the competition between the short- and long-range interactions in 1D systems determines the type and the temperature of the spin transitions and, where relevant, the width of the hysteresis loop. The model describes successfully the main features of the pressure effect in 1D spin crossover systems. When short-range interactions significantly exceed long-range interactions, the width of the hysteresis loop is only slightly influenced by pressure, whereas the mean value of the transition temperature increases significantly with pressure. Thus pressure studies of 1D systems provide information about the strength of short- and long-range interactions.

6.2. 2D spin crossover systems

Only a few two-dimensional (2D) spin crossover compounds have been reported in the literature up to now. Most of them belong to the series of $[FeL_2(NCS)_2]\cdot n$S, where L is a bis-monodentate ligand. One member of this family was prepared by Haasnoot from L = 4,4′-bitriazole (btr) [53(a) and (b)]. The N2,N4 and N1,N1′ bridging modes of btr ligands lead to a 2D layered compound of composition $[Fe(btr)_2(NCS)_2]\cdot H_2O$ (Fig. 22). In this system, the iron(II) ions are surrounded by four nitrogen atoms belonging to the triazole rings, and two thiocyanate anions fill the apical positions of the compressed octahedron. The layers are interconnected by means of van der Waals forces and weak hydrogen bonds involving the non-coordinating water molecules.

At atmospheric pressure, this compound displays an abrupt ST at low temperatures with hysteresis [62], this latter behaviour being probably due to a crystallographic phase transition [63]. Where, as is likely in this instance, both a spin

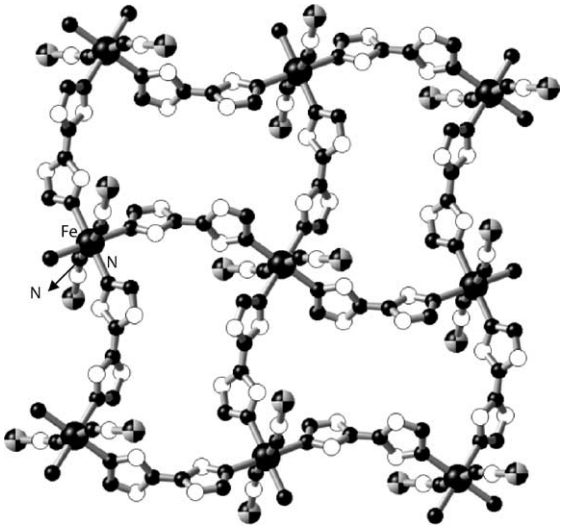

Fig. 22. Molecular structure of the polymeric complex $[Fe(btr)_2(NCS)_2]\cdot H_2O$, (adapted from [22]).

transition and a crystallographic phase transition occur, the pressure dependence of both phenomena can be followed, and in the most favourable cases a decoupling can be observed between them [64]. In Fig. 23 the magnetic response of the material in the form of $\chi_M T$ versus T at different pressures is illustrated. The main features observed with increasing pressure are: (i) the spin transitions in both cooling and warming modes become less abrupt and are shifted towards higher temperatures; (ii) the hysteresis width decreases and finally disappears at ca. 1 GPa, where the system unexpectedly shows a considerable stabilisation of the HS state under pressure; (iii) after pressure release the hysteresis is essentially restored, but a considerable amount of HS fraction remains in the low temperature region, which finally relaxes (after 175 h at room temperature) to a steady value of ∼30%.

These observations demonstrate that it is possible to induce a complete LS → HS conversion by applying hydrostatic pressure to an iron(II) ST material. This is entirely unexpected since normally an increase of pressure stabilises the low spin state. The appearance of the HS state under pressure was earlier observed on LS iron(II) complexes by Mössbauer spectroscopy and, as stated before, was probably due to non-hydrostatic conditions [9,31,65]. The possibility of converting LS to HS by applying pressure was theoretically considered by Kambara [66]. He proposed that the HS state can be stabilised by increasing the intramolecular coupling strength by pressure, since the molecular displacements with E_g symmetry can couple only with the HS state. The experimentally observed pressure dependence of the HS fraction for the present compound cannot be described by this model, probably because the cooperative interactions that are relevant in the present case were not considered in this theory.

We assume that in the present case the ST is triggered by a crystallographic phase transition, in contrast to $[Fe(ptz)_6](BF_4)_2$ where the ST triggers the crystallographic phase transition [67]. The isostructural com-

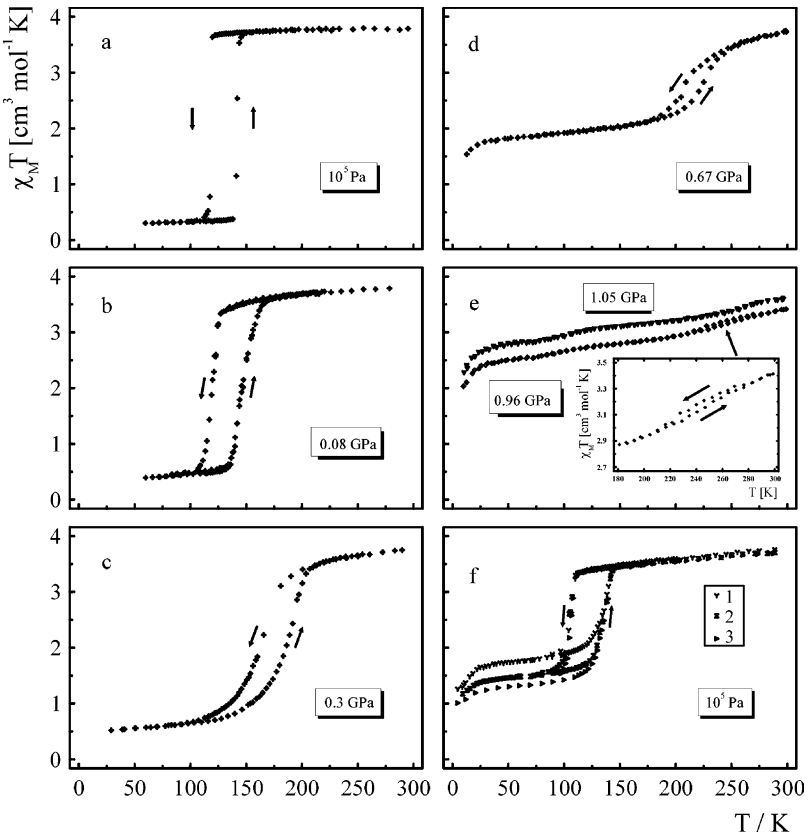

Fig. 23. $\chi_M T$ vs. T curves at different pressures for $[Fe(btr)_2(NCS)_2]\cdot H_2O$, (adapted from [62]).

pound $[Fe(btre)_2(NCS)_2]$ with btre = 1,2-bis(1,2,4-triazol-4-yl)ethane remains HS even at 1.2 GPa [68]. Its crystal structure does not reveal any hydrogen bonds in contrast to that of $[Fe(btr)_2(NCS)_2]\cdot H_2O$. This might play a decisive role in the appearance of the structural phase transition and thus of the spin crossover behaviour in the latter compound.

We aim to clarify this behaviour further by X-ray measurements at variable temperatures and pressures and to establish the phase diagram of $[Fe(btr)_2(NCS)_2]\cdot H_2O$ in order to specify the variety of structural modifications induced by pressure.

The spin transition in $[Fe(btr)_2(NCS)_2]\cdot H_2O$, neat and diluted in a Ni-homologue, was recorded using optical reflectivity in the pressure range up to 0.16 GPa [69]. The observed variation of the transition temperature with pressure was higher in comparison with magnetic susceptibility measurements. It is likely that this discrepancy originates from

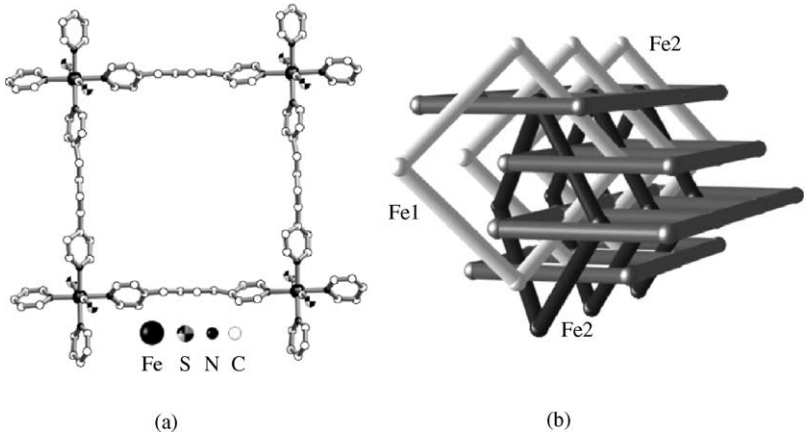

Fig. 24. Molecular structure of $[Fe(bpb)_2(NCS)_2]\cdot 0.5$ MeOH (a). Schematic view of the triple interpenetration of the $[Fe(bpb)_2(NCS)_2]_n$ grids. The parallel A set of planes, defined by iron atoms of the type Fe1, is interpenetrated by the mutually interpenetrated B and C sets of planes, which are defined by the iron atom of the type Fe2 (see text) (b), (adapted from [70]).

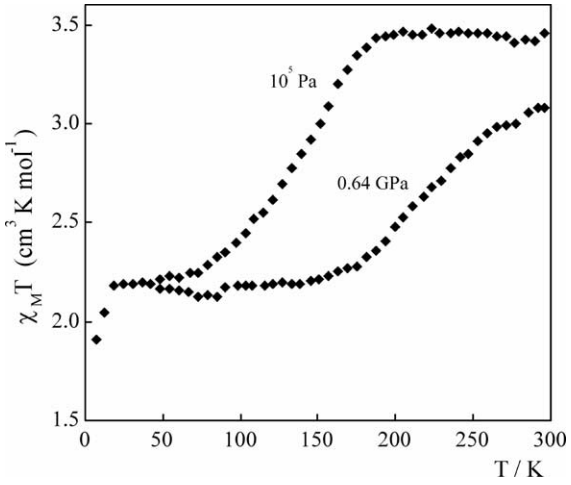

Fig. 25. $\chi_M T$ vs. T curves at different pressures for $[Fe(bpb)_2(NCS)_2]\cdot 0.5$ MeOH, (adapted from [71]).

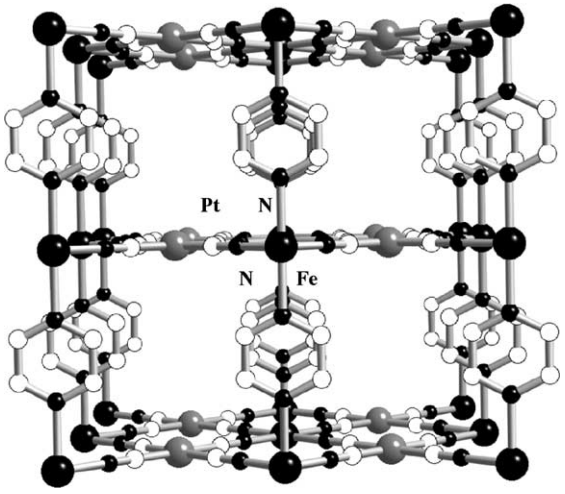

Fig. 26. Perspective view of the 3D coordination polymer $\{[Fe(pz)_2[Pt(CN)_4]\}\cdot 2H_2O$, (adapted from [22]).

the different SCO behaviour on the surface as compared to the bulk.

Real and co-workers have reported on a new 2D spin crossover system formulated as $[Fe(bpb)_2(NCS)_2]\cdot 0.5$ MeOH (bpb = 1,4-bis(4-piridyl)butadiyne) which consists of two different arrays of nets (Fig. 24). Two crystallographically independent iron sites (Fe1 and Fe2) define the nodes of the nets [70]. The iron atoms have similar coordination surroundings in both sites, which consist of compressed octahedra with two trans-thiocyanato ligands in the axial positions and four pyridine N-atoms in the basal plane. Each bpb ligand connects two iron atoms defining large [Fe4] squares (Fig. 24). The edge-shared squares define the net structures with all the iron atoms, either coplanar (A set, Fe1) or slightly corrugated (B set, Fe2). The iron-to-iron separation through the bpb ligand is 16.628 and 16.393 Å for the A and B nets, respectively. B consists of two mutually perpendicular stacks of inter-locked squared grids organised along [1 1 0] and [−1 1 0] directions. These two stacks also interpenetrate the A set giving an unprecedented supramolecular architecture formed by three mutually perpendicular interpenetrated nets. In Fig. 25 are depicted the $\chi_M T$ versus T curves for $[Fe(bpb)_2(NCS)_2]\cdot 0.5$ MeOH at two different pressures [60,71]. At 0.64 GPa 50% of the transition is still retained but $T_{1/2}$ is shifted upwards. The continuous character of the spin transition becomes more pronounced and a LS fraction at 300 K is inferred from the value of $\chi_M T$ at this temperature. Further increase of pressure, even up to 1.14 GPa, has no further effect. This indicates a barrier to spin change at the Fe2 site and the concomitant change in volume which presumably cannot be accommodated in this highly interlocked network structure.

6.3. 3D spin crossover systems

Few 3D polymeric SCO systems have been synthesised and structurally characterised [72,73]. Most of these systems possess perchlorate as counterions, and due to the danger in working with these under pressure, no pressure studies have been done so far. A new series of 3D spin crossover compounds has been obtained by extension of the $\{[Fe(py)_2[M(CN)_4]\}$ 2D system where py = pyridine and M is Ni(II), Pd(II) or Pt(II) [53f]. Replacement of the py ligand by pz (pyrazine) in the 2D system affords the new family of 3D compounds $\{[Fe(pz)_2[M(CN)_4]\}\cdot 2H_2O$. The molecular structure is illustrated in Fig. 26. The pz ligand bridges the iron atoms of consecutive sheets achieving a pillaring of the

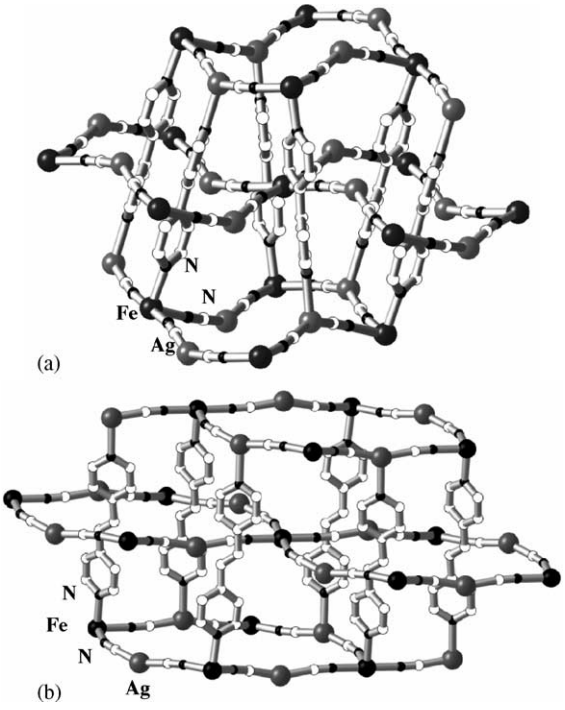

Fig. 27. View of the interpenetrating double framework structure of $\{Fe(4,4'\text{-bipy})_2[Ag(CN)_2]_2\}$ (a) and $\{Fe(bpe)_2[Ag(CN)_2]_2\}$ (b), (adapted from [53c]).

2D sheets by vertical columns of the pz bridge to give the 3D structure. These compounds undergo strong cooperative spin transition with 20–40 K wide hysteresis loops at ambient pressure. Molnar et al. have recorded the solid-state Raman spectra at room temperature as a function of pressure [26]. The studies show a reproducible pressure induced hysteresis loop at room temperature for the Ni derivative. For the Pd and Pt complexes, the spin state change occurs between 0.18 and 0.35 GPa, respectively, and competes with a pressure-induced structural transformation.

Concurrently with the synthesis of these polymers, Real and co-workers [53c] have investigated the suitability of the $[Ag(CN)_2]^-$ anion for the synthesis of new 3D spin crossover systems. Using 4,4′-bipy and bpe (bispyridylethylene) as bridging ligands they have succeeded to synthesise two new 3D molecular architectures with interesting magnetic response under hydrostatic pressure. In Fig. 27 are depicted a perspective view of the interpenetrating double framework structure of $\{Fe(4,4'\text{-bipy})_2[Ag(CN)_2]_2\}$ and $\{Fe(bpe)_2[Ag(CN)_2]_2\}$. The crystal structures of both derivatives are very similar and complicated. The axial positions of each iron atom are occupied by two organic bridging ligands which link two Ag atoms belonging to alternate $\{Fe_4[Ag(CN)_2]_4\}_n$ layers so that each $\{Fe_4[Ag(CN)_2]_4\}$ window of contiguous layers is threaded twice by the organic bridges. The average Fe–N bond length in $\{Fe(4,4'\text{-bipy})_2[Ag(CN)_2]_2\}$ is 0.011(9) Å greater than that for $\{Fe(bpe)_2[Ag(CN)_2]_2\}$ in the high spin state. This small difference agrees with the fact that the former complex is HS in the whole range of temperatures studied while the latter undergoes thermal spin transition at ambient pressure (see Fig. 28). The thermal spin conversion induced under pressure for $\{Fe(4,4'\text{-bipy})_2[Ag(CN)_2]_2\}$ takes place without thermal hysteresis, being similar to that observed for $\{Fe(bpe)_2[Ag(CN)_2]_2\}$ in the crystalline form. When pressure increases, a continuous and incomplete spin transition is observed which is shifted upwards to higher temperatures. Furthermore, the low temperature HS residual fraction decreases. Finally, at ca. 0.6 GPa the spin transition disappears and the system is stabilised in the LS state at all temperatures studied. The $\{Fe(bpe)_2[Ag(CN)_2]_2\}$ system exhibits thermal spin transition at ambient pressure but only in half the iron (II) centers. The sharp decrease of $\chi_M T$ after the plateau arises from the ZFS of the remaining iron(II) ions in the HS state. The spin crossover behaviour in this system turns out to be very susceptible to pressure. As seen in Fig. 28 pressure of only ca. 0.5 GPa seems to be sufficient to stabilise the system in the LS state. The plot of $\chi_M T$ at 300 K versus P for $\{Fe(4,4'\text{-bipy})_2[Ag(CN)_2]_2\}$ (Fig. 29) shows the unusual discontinuous character of the pressure-induced spin transition at room temperature. Although no hysteresis is observed, the extreme sensitivity of $\{Fe(4,4'\text{-bipy})_2[Ag(CN)_2]_2\}$ and $\{Fe(bpe)_2[Ag(CN)_2]_2\}$ to pressure at 300 K suggests the occurrence of strong cooperativity in the 3D network.

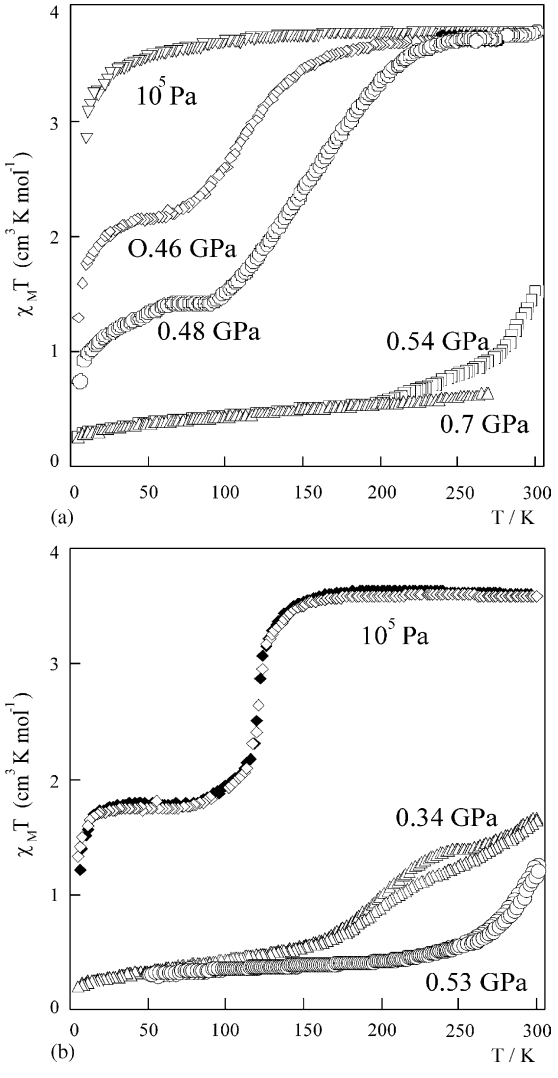

Fig. 28. $\chi_M T$ vs. T curves at different pressures for $\{Fe(4,4'\text{-bipy})_2[Ag(CN)_2]_2\}$ (a) and $\{Fe(bpe)_2[Ag(CN)_2]_2\}$ (b), (adapted from [53c]).

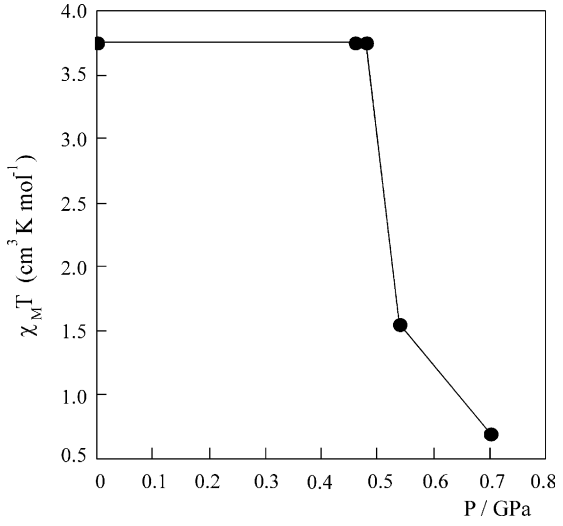

Fig. 29. Plot of $\chi_M T$ vs. P at 300 K for $\{Fe(4,4'\text{-bipy})_2[Ag(CN)_2]_2\}$, (adapted from [53c]).

7. Conclusions

The results of pressure effect studies in solid-state on spin crossover compounds using hydrostatic pressure cells and magnetic susceptibility and Mössbauer effect measurements have been presented and discussed. It has been demonstrated that the application of pressure provides important information on thermodynamical properties and on the driving force of thermal spin transition in SCO compounds. Analysing the evolution of the spin transition curve obtained under pressure allows to extract, along with the changes of enthalpy and entropy, the change of the volume of the unit cell ΔV upon spin conversion as well as the behaviour of the interaction constant Γ. It is also shown that application of pressure is a powerful tool to investigate the role of the structure and the interplay between spin transition and structural phase transition. Changes of the molecular volumes play a significant role in the cooperative interactions in solid compounds exhibiting dynamical electronic structures such as in spin crossover. Application of pressure is an elegant method of changing the ligand field strength and thereby modifying the spin transition behaviour in a controlled manner. The influence of hydrostatic pressure on mono-, oligo- and polynuclear SCO systems has yielded results which are, on the one hand, quite expected like the stabilisation of the LS state due to its smaller molecular volume as compared to that of the HS state. On the other hand, some unexpected features in the SCO behaviour have been observed under pressure which await quantitative theoretical interpretation. There are, for instance, the two types of pressure influence: (i) the shape of the ST curve remains essentially unchanged, but is shifted parallel to higher temperatures under pressure; (ii) the relatively steep ST curve at ambient pressure becomes more and more gradual, stabilising the LS state and shifting $T_{1/2}$ upwards, as pressure increases, until the HS state entirely disappears. In both cases it is, of course, the molecular volume change ΔV_{HL} that tends to stabilise the LS state under pressure. But there must be other factors, most probably arising from special lattice properties (hydrogen bonding, π–π stacking, packing effects), which are held responsible for the cooperative interactions between the spin state changing molecules and also contribute to the pressure-induced changes of the SCO behaviour. By the same token, it is believed that the unexpected stabilisation of the HS state and gradual diminishing of the hysteresis with increasing pressure seen in some cases have their origin in particular lattice properties. Clearly, theoretical progress in understanding such unexpected pressure effects will only be possible with data from crystal structure determination under applied pressure and, of course, variable temperature.

Acknowledgements

We thank the European Commission for granting the TMR-Network “Thermal and Optical Switching of Molecular Spin States (TOSS)”, Contract No. ERB-FMRX-CT98-0199EEC/TMR. Financial support from the Deutsche Forschungsgemeinschaft, the Fonds der Chemischen Industrie and the Materialwissenschaftliches Forschungszentrum of the University of Mainz is gratefully acknowledged. A.B.G. is grateful for a fellowship from Alexander von Humboldt Foundation. We thank Prof. J.A. Real for making available structural data.

References

[1] A.H. Ewald, R.L. Martin, E. Sinn, A.H. White, Inorg. Chem. 8 (1969) 1837.
[2] E. König, Ber. Bunsenges. Phys. Chem. 76 (1972) 975.
[3] H.G. Drickamer, C.W. Frank, Electronic Transitions and the High Pressure Chemistry and Physics of Solids, Chapman & Hall, London, 1973.
[4] D.M. Adams, G.J. Long, A.D. Williams, Inorg. Chem. 21 (1982) 1049.
[5] J. Pebler, Inorg. Chem. 22 (1983) 4125.
[6] E. König, G. Ritter, S.K. Kulshreshtha, J. Waigel, H.A. Goodwin, Inorg. Chem. 23 (1984) 1896.
[7] S. Usha, R. Srinivasan, C.N.R. Rao, Chem. Phys. 100 (1985) 447.
[8] E. Meissner, H. Köppen, C.P. Köhler, H. Spiering, P. Gütlich, Hyperfine Interact. 36 (1987) 1.
[9] G.L. Long, B.B. Hutchinson, Inorg. Chem. 26 (1987) 608.
[10] J.K. McCusker, M. Zvagulis, H.G. Drickamer, D.N. Hendrickson, Inorg. Chem. 28 (1989) 1380.
[11] M. Konno, M. Mikami-Kido, Bull. Chem. Soc. Jpn. 64 (1991) 339.
[12] (a) C.P. Köhler, R. Jakobi, E. Meissner, L. Wiehl, H. Spiering, P. Gütlich, J. Phys. Chem. Solids 51 (1990) 239;
(b) T. Kohlhaas, H. Spiering, P. Gütlich, Z. Physik. B 102 (1997) 455;
(c) H. Romstedt, A. Hauser, H. Spiering, J. Phys. Chem. Solids 59 (1998) 265.
[13] P. Adler, H. Spiering, P. Gütlich, Hyperfine Interact. 42 (1988) 1035.
[14] (a) P. Gütlich, A. Hauser, H. Spiering, Angew. Chem. Int. Ed. Engl. 33 (1994) 2024;
(b) P. Gütlich, H.A. Goodwin (Eds.), Spin Crossover Transition Metal Compounds, Springer, vol. 233–235, Top. Curr. Chem., 2004.
[15] E.W. Müller, H. Spiering, P. Gütlich, Chem. Phys. Lett. 93 (1982) 567.
[16] E. König, G. Ritter, J. Waigel, H.A. Goodwin, J. Chem. Phys. 83 (1985) 3055.
[17] V. Ksenofontov, H. Spiering, A. Schreiner, G. Levchenko, H.A. Goodwin, P. Gütlich, J. Phys. Chem. Solids 60 (1999) 393.
[18] V. Ksenofontov, G. Levchenko, S. Reiman, P. Gütlich, A. Bleuzen, V. Escax, M. Verdaguer, Phys. Rev. B 68 (2003) 024415.
[19] G.J. Long, L.W. Becker, B.B. Hutchinson, Adv. Chem. Ser. 194 (1981) 453.
[20] P. Guionneau, C. Brigouleix, Y. Barrans, A.E. Goeta, J.F. Létard, J. Howard, J. Gaultier, D. Chasseau, C.R. Acad. Sci. IIC 4 (2001) 161.
[21] T. Granier, B. Gallois, J. Gaultier, J.A. Real, J. Zarembowitch, Inorg. Chem. 32 (1993) 5305.
[22] J.A. Real, A.B. Gaspar, V. Niel, M.C. Muñoz, Coord. Chem. Rev. 236 (2003) 121.
[23] C. Hannay, M.J. Hubin-Franskin, F. Grandjean, V. Briois, J.P. Itie, A. Polian, S. Trofimenko, G.J. Long, Inorg. Chem. 36 (1997) 5580.
[24] C. Piquer, F. Grandjean, O. Mathon, S. Pascarelli, D.L. Reger, C.A. Little, G.J. Long, Inorg. Chem. 42 (2003) 982.
[25] D.M. Adams, G.J. Long, A.D. Williams, Inorg. Chem. 21 (1982) 1049.
[26] G. Molnar, V. Niel, J.A. Real, L. Dubrovinsky, A. Bousseksou, J.J. McGarvey, J. Phys. Chem. B 107 (2003) 3149.

[27] J. Jeftić, R. Hinek, S.C. Capelli, A. Hauser, Inorg. Chem. 36 (1997) 3080.
[28] J. Jeftić, N. Menéndez, A. Wack, E. Codjovi, J. Linarès, A. Goujon, G. Hamel, S. Klotz, G. Syfosse, F. Varret, Meas. Sci. Technol. 10 (1999) 1059.
[29] M. Baran, G.G. Levchenko, V.P. Dyakonov, G. Shymchak, Phys. C 241 (1995) 383.
[30] K. Madeja, E. König, J. Inorg. Nucl. Chem. 25 (1963) 377.
[31] D.C. Fisher, H.G. Drickamer, J. Chem. Phys. 54 (1971) 4825.
[32] (a) P. Ganguli, P. Gütlich, E.W. Müller, Inorg. Chem. 21 (1982) 3249;
(b) B. Gallois, J.A. Real, C. Hauw, J. Zarembowitch, Inorg. Chem. 29 (1990) 1152.
[33] (a) V. Ksenofontov, A.B. Gaspar, G. Levchenko, B. Fitzsimmons, P. Gütlich, J. Phys. Chem. B 108 (2004) 7723;
(b) P. Gütlich, A.B. Gaspar, V. Ksenofontov, Y. Garcia, J. Phys. Cond. Matter. 16 (2004) S1087.
[34] (a) E. Meissner, H. Köppen, H. Spiering, P. Gütlich, Chem. Phys. Lett. 95 (1983) 163;
(b) H. Spiering, E. Meissner, H. Köppen, E.W. Müller, P. Gütlich, Chem. Phys. 68 (1982) 65;
(c) P. Adler, L. Wiehl, E. Meissner, C.P. Köhler, H. Spiering, P. Gütlich, J. Phys. Chem. Solids 48 (1987) 517.
[35] D.M. Halepoto, D.G.L. Holt, L.F. Larkworthy, G.L. Leigh, D.C. Povey, G.W. Smith, J. Chem. Soc. Chem. Commun. (1989) 1322.
[36] (a) J. Kusz, H. Spiering, P. Gütlich, J. Appl. Cryst. 34 (2001) 229;
(b) J. Kusz, P. Gütlich, H. Spiering, in: P. Gütlich, H.A. Goodwin (Eds.), Spin Crossover Transition Metal Compounds, Springer, Top. Curr. Chem. 234 (2004) 129.
[37] V. Ksenofontov, G.G. Levchenko, H. Spiering, P. Gütlich, J.F. Lètard, Y. Bouhedja, O. Kahn, Chem. Phys. Lett. 294 (1998) 545.
[38] V. Ksenofontov, A.B. Gaspar, P. Gütlich, in: P. Gütlich, H.A. Goodwin (Eds.), Spin Crossover in Transition Metal Compounds, Springer, Top. Curr. Chem. 235 (2004) 23.
[39] (a) L. Wiehl, Acta Cryst. B49 (1993) 289;
(b) L. Wiehl, H. Spiering, H. Gütlich, K. Knorr, J. Appl. Cryst. 23 (1990) 151.
[40] P. Poganiuch, S. Decurtins, P. Gütlich, J. Am. Chem. Soc. 112 (1990) 3270.
[41] (a) A.B. Gaspar, M.C. Muñoz, N. Moliner, V. Ksenofontov, G.G. Levchenko, P. Gütlich, J.A. Real, Monatsh. Chem. 134 (2003) 285;
(b) A.B. Gaspar, M.C. Muñoz, N. Moliner, V. Ksenofontov, G.G. Levchenko, P. Gütlich, J.A. Real, in: W. Linert, M. Verdaguer (Eds.), Molecular Magnets. Recent Highlights, 169, Springer-Verlag, Wien, New York, 2003, p. 178.
[42] E. König, G. Ritter, H. Grünsteudel, J. Dengler, J. Nelson, J. Inorg. Chem. 33 (1994) 837.
[43] C. Bruns-Yilmaz, Ph.D. Thesis, University of Mainz, Germany, 1999.
[44] A.N. Das, B. Ghos, J. Phys. C: Solid State Phys. 16 (1983) 1799.
[45] (a) N. Willenbacher, H. Spiering, J. Phys. C. 21 (1988) 1423;
(b) H. Spiering, N. Willenbacher, J. Phys. Condens. Matter. 1 (1989) 10089.
[46] J.D. Eshelby, Solid State Phys. 3 (1956) 79.
[47] G.G. Levchenko, V. Ksenofontov, A.V. Stupakov, H. Spiering, Y. Garcia, P. Gütlich, Chem. Phys. 277 (2002) 125.
[48] (a) L.R. Dalton, A.W. Harper, R. Ghosn, W.H. Steier, M. Ziari, H. Fetterman, Y. Shi, R.W. Mustacich, A.K.Y. Jen, K.J. Shea, Chem. Mater. 7 (1995) 1060;
(b) R. Dagani, Chem. Eng. News 4 (1996) 22.
[49] J.A. Real, A.B. Gaspar, M.C. Muñoz, P. Gütlich, V. Ksenofontov, H. Spiering, in: P. Gütlich, H.A. Goodwin (Eds.), Spin Crossover in Transition Metal Compounds, Springer, Top. Curr. Chem. 233 (2004) 167.
[50] J.A. Real, H. Bolvin, A. Bousseksou, A. Dworkin, O. Kahn, F. Varret, J. Zarembowitch, J. Am. Chem. Soc. 114 (1992) 4650.
[51] V. Ksenofontov, A.B. Gaspar, J.A. Real, P. Gütlich, J. Chem. Phys. B 105 (2001) 12266.
[52] A.B. Gaspar, V. Ksenofontov, H. Spiering, S. Reiman, J.A. Real, P. Gütlich, Hyperfine Interact. 144/145 (2002) 297.
[53] (a) J.G. Haasnoot, W.L. Groeneveld, Z. Naturforsch. 346 (1979) 1500;
(b) J.G. Haasnoot, Coord. Chem. Rev. 200–202 (2000) 131;
(c) V. Niel, M.C. Muñoz, A.B. Gaspar, A. Galet, G. Levchenko, J.A. Real, Chem. Eur. J. 11 (2002) 2446;
(d) J.A. Real, E. Andrés, M.C. Muñoz, M. Julve, T. Trainer, A. Bousseksou, Science 268 (1995) 265;
(e) G.J. Halder, C.J. Kepert, B. Mourabaki, K.S. Murray, J.D. Cashion, Science 298 (2002) 1762;
(f) V. Niel, J.M. Martinez-Agudo, A.B. Gaspar, M.C. Muñoz, J.A. Real, Inorg. Chem. 40 (2001) 3838;
(g) V. Niel, A. Galet, A.B. Gaspar, M.C. Muñoz, J.A. Real, Chem. Commun. 1248 (2003).
[54] (a) L.G. Lavrenova, V.N. Ikorskii, V.A. Varnek, I.M. Oglezneva, S.V. Larionov, Koord. Kim. 12 (1986) 207;
(b) L.G. Lavrenova, V.N. Ikorskii, V.A. Varnek, I.M. Oglezneva, S.V. Larionov, J. Struct. Chem. 34 (1993) 960;
(c) L.G. Lavrenova, L.G. Yudina, V.N. Ikorskii, V.A. Varnek, I.M. Oglezneva, S.V. Larionov, Polyhedron 14 (1995) 1333.
[55] (a) J. Kröber, E. Codjovi, O. Kahn, F. Grolière, C. Jay, J. Am. Chem. Soc. 115 (1993) 9810;
(b) E. Codjovi, L. Sommier, O. Kahn, C. Jay, New J. Chem. 20 (1996) 503;
(c) O. Kahn, C.J. Martinez, Science 279 (1998) 44.
[56] A. Michalowicz, J. Moscovici, B. Ducourant, D. Cracco, O. Kahn, Chem. Mater. 7 (1995) 1833.
[57] Y. García, V. Ksenofontov, P. Gütlich, Hyperfine Interact. 139/140 (2002) 543.
[58] Y. García, P.J. van Koningsbruggen, R. Lapouyade, L. Fournés, L. Rabardel, O. Kahn, V. Ksenofontov, G.G. Levchenko, P. Gütlich, Chem. Mater. 10 (1998) 2426.
[59] N. Moliner, M.C. Muñoz, S. Létard, L. Salmon, J.P. Tuchagues, A. Bousseksou, J.A. Real, Inorg. Chem. 41 (2002) 6997.
[60] A.B. Gaspar, Ph.D. Thesis, Valencia, 2002.
[61] S. Klokishner, J. Linarès, F. Varret, Chem. Phys. 255 (2000) 317.
[62] Y. García, V. Ksenofontov, G.G. Levchenko, G. Schmitt, P. Gütlich, J. Phys. Chem. B 104 (2000) 5045.
[63] (a) W. Vreugdenhil, J.H. van Diemen, R.A.G. de Graff, J.G. Haasnoot, J. Reedijk, A. van der Kraan, O. Kahn, J. Zarembowitch, Polyhedron 9 (1990) 2971;
(b) A. Ozarowski, Y. Shunzhong, B.R. McGarvey, A. Mislankar, J.E. Drake, Inorg. Chem. 30 (1991) 3167;
(c) J.P. Martin, J. Zarembowitch, A. Dworkin, J.G. Haasnoot, E.C. Codjovi, Inorg. Chem. 33 (1994) 2617.
[64] J. Jeftic, A. Hauser, J. Phys. Chem. B 101 (1997) 10262.
[65] C.P. Slichter, H.G. Drickamer, J. Chem. Phys. 56 (1972) 2142.
[66] T. Kambara, J. Phys. Soc. Jpn. 50 (1981) 2257.
[67] (a) J. Jung, G. Schmitt, L. Wiehl, A. Hauser, K. Knorr, H. Spiering, P. Gütlich, Z. Phys. B 100 (1996) 523;
(b) J. Jeftic, H. Romstedt, A. Hauser, J. Phys. Chem. Solids 57 (1996) 1743.
[68] Y. García, V. Ksenofontov, G. Bravic, D. Chasseau, P. Gütlich, unpublished results.
[69] E. Codjovi, N. Menéndez, J. Jeftic, F. Varret, C.R. Acad. Sci. Ser. IIC Chem. 4 (2001) 181.
[70] N. Moliner, M.C. Muñoz, S. Létard, X. Solans, N. Menéndez, A. Goujon, F. Varret, J.A. Real, Inorg. Chem. 39 (2000) 5390.
[71] A.B. Gaspar, V. Ksenofontov, J.A. Real, P. Gütlich, unpublished results.
[72] Y. García, O. Kahn, L. Rabardel, L. Chansou, L. Salmon, J.P. Tuchagues, Inorg. Chem. 38 (1999) 4663.
[73] P.J. van Koningsbruggen, Y. García, H. Kooijman, A.L. Spek, J.G. Haasnoot, O. Kahn, J. Linarès, E. Codjovi, F. Varret, J. Chem. Soc. Dalton Trans. (2001) 466.